Correlation of Simultaneous Differential Gene Expression in the Blood and Heart with Known Mechanisms of Adriamycin-Induced Cardiomyopathy in the Rat

H. Roger Brown, Hong Ni, Gina Benavides, Lawrence Yoon, Karim Hyder, Jaisri Giridhar, Guy Gardner, Ronald D. Tyler and Kevin T. Morgan

Toxicol Pathol 2002 30: 452
DOI: 10.1080/01926230290105604

TOXICOLOGIC PATHOLOGY, vol 30, no 4, pp 452–469, 2002

DOI: 10.1080/01926230290105604

Correlation of Simultaneous Differential Gene Expression in the Blood and Heart with Known Mechanisms of Adriamycin-Induced Cardiomyopathy in the Rat

H. ROGER BROWN,[1] HONG NI,[1] GINA BENAVIDES,[1] LAWRENCE YOON,[1] KARIM HYDER,[3] JAISRI GIRIDHAR,[2] GUY GARDNER,[2] RONALD D. TYLER,[1] AND KEVIN T. MORGAN[1]

[1]*Drug Safety, Toxicogenomics, GlaxoSmithKline, Inc, Research Triangle Park, North Carolina 27709*
[2] *Medicine Safety Evaluation, GlaxoSmithKline, Inc, Research Triangle Park, North Carolina 27709, and*
[3]*Clontech Laboratories, Inc, Palo Alto, California 94303*

ABSTRACT

As the genomes of mammalian species become sequenced and gene functions are ascribed, the use of differential gene expression (DGE) to evaluate organ function will become common in the experimental evaluation of new drug therapies. The ability to translate this technology into useful information for human exposures depends on tissue sampling that is impractical or generally not possible in man. The possibility that the DGE of nucleated cells, reticulocytes, or platelets in blood may present the necessary link with target organ toxicity provides an opportunity to correlate preclinical with clinical outcomes. Adriamycin is highly effective alone and more frequently in combination with other chemotherapeutic agents in the treatment of a variety of susceptible malignancies. Adriamycin-induced cardiomyopathy was examined as an endpoint to measure the utility of DGE on whole blood as a predictor of cardiac toxicity. Statistically significant gene changes were observed between relevant blood and cardiac gene profiles that corroborated the accepted mechanisms of toxicity (oxidative stress, effects on carnitine transport, DNA intercalation). There were, however, clear indications that other target organs (bone marrow and intestinal tract) were affected. The divergent expression of some genes between the blood and the heart on day 7 may also indicate the timing and mechanism of development of the cardiomyopathy and confirm current therapeutic approaches for its prevention. The data demonstrate that whole blood gene expression particularly in relation to oxidative stress, in conjunction with standard hematology and clinical chemistry, may be useful in monitoring and predicting cardiac damage secondary to adriamycin administration.

Appendices A & B, referenced in this paper, are not printed in this issue of *Toxicologic Pathology*. They are available as downloadable text files at http://taylorandfrancis.metapress.com/openurl.asp?genre=journal&issn=0192-6233. To access them, click on the issue link for 30(4), then select this article. A download option appears at the bottom of this abstract. In order to access the full article online, you must either have an individual subscription or a member subscription accessed through www.toxpath.org.

Keywords. Blood; heart; gene expression; doxorubicin.

INTRODUCTION

Therapeutic agents, and particularly anticancer chemotherapies, carry the promise of effective treatments and perhaps cures for the disease entities targeted. However, a successful treatment may also entail added burdens at the molecular, tissue, and organ levels that may lead to cellular, tissue, and organ damage as an unavoidable consequence. In the face of malignancy, the risk-to-benefit ratio may seem obvious. For a variety of disease entities, knowing the risk by monitoring both the disease progression as well as the cumulative damage from the therapy, necessitates a continuing reassessment by the physician of whether a specific therapy continues. Blood profiling of clinical chemistry parameters has, over a prolonged period of development, provided valuable information about disease progression and physiologic function of most of the organs of the body. However, the mechanistic pathways leading to the observed changes and the time course involved are often obscured once the lesion is detectable. The presence of sufficient numbers of nucleated cells (predominantly neutrophils, lymphocytes, and monocytes) in the blood offers the opportunity to use blood as a tissue for differential gene expression (DGE). The contribution of platelets (1) and reticulocytes (2) to gene expression will need to be examined further as both contain residual transcripts reflecting precursor responses in the bone marrow. DGE reveals relative changes in mRNA transcript levels in control vs treated cell populations. DGE can provide insight into both the current molecular state of the population and clues as to the mechanisms by which known perturbations occur. Sequential sampling also provides the opportunity to detect divergences from the normal state. The timing of those divergences can be compared against biochemical substrates and endogenous protectants to identify possible interventions that will reverse or prevent consequential damage. For this premise to be meaningful, the therapeutic agent must (a) target responses in the genome that are common between the first cells to "see" the agent (blood) and the cells of the definitive target organs, and then (b) induce shared transcriptional responses (not necessarily translational and biochemical) that are indicators of events that lead to toxicity in the target organ(s) by virtue of specific inadequacies of protection or exaggerated needs or responses of the tissue.

Clearly not all therapeutic agents will lend themselves to this type of evaluation but the extent to which DGE can be used in this fashion is clearly only now being evaluated and the understanding of the uses and limitations of the technology is embryonic. To test the value of blood

Address correspondence to: H. Roger Brown, GlaxoSmithKline, Inc, Mai. T 1158, Five Moore Drive, Research Triangle Park, NC, 27709; e-mail: hrb25873@gsk.com

0192-6233/02$3.00+$0.00

DGE as a surrogate for detecting toxicity in other organs we exposed rats to weekly adriamycin treatment by IP injection, at doses reported to lead to adriamycin-induced cardiomyopathy. Clontech cDNA gene arrays were used to measure DGE in both the blood and hearts of treated and control animals. Blood and tissues were sampled 4 hours after the initial dose and 24 hours after dosing on days 1, 8, and 38. At the end of the 38-day period there was clear histopathologic evidence of adriamycin-induced cardiomyopathy. Genes differentially expressed on days 1 and 8 in both the blood and heart consistently pointed to known mechanisms of adriamycin-induced toxicity. Beginning on day 8 there were key gene divergences between the heart and blood that may indicate the point at which the heart is committed to a cardiomyopathic state. Other sites of adriamycin toxicity were also indicated by the specific gene patterns expressed.

MATERIALS AND METHODS

In Vivo Measurements

Four-to-5-month-old male rats [Crl:WI(Glx/BRL/Han) IGSBR] Taconic, Germantown, NY, USA] were housed on stainless steel wire mesh, suspension cages (1 per cage). Animals were maintained at a temperature of 64–79°F, relative humidity of 30–70%, 12 hours light/dark cycle, 10–15 room air changes per hour, and were fed ad libitum Certified Rodent Diet 5002 pellets (PMI Feeds) and reverse osmosis/UV light-treated water. All animals were observed at least twice daily for mortality and moribundity. Clinical observations were recorded at least twice daily for all animals during the treatment period of the study. All experiments were performed using protocols approved by the GlaxoSmithKline Institutional Animal Care and Use Committee. A brief summary of the study design and dosing schedule is presented in Table 1.

Three rats per group were injected intraperitoneally with adriamycin hydrochloride (adriamycin PFS, Pharmacia UpJohn) at a dose of 4.0 mg/kg/week (considered to approximate a toxic but therapeutic dose) or 15.0 mg/kg as a single dose (acutely toxic and producing cardiomyopathy as a fractionated dose) on day 1. A third set of 5 animals per group received a second intraperitoneal injection at 4.0 mg/kg 1 week after the first injection. The remaining treated group of 5 animals per group received weekly injections of 4 mg/kg for up to 4 total doses (4.8 mg total dose-euthanasia at 38 days). Control animals were injected with saline adjusted to the pH of the adriamycin solution. The intraperitoneal route of administration on a once-per-week basis was chosen based on reports by Doroshow et al (3) as to the rapid time course of heart failure by this method. Sampling times of 24 hours, 8 days, and 38 days were based on these same reports and efforts to sample early, intermediate, and late changes in gene expression. Body weights were taken on 3 occasions prior to initiation of treatment and were used in conjunction with serum insulin and glucose levels to assign animals to equal groups. Body weights were then taken on a weekly basis and at the termination of the study. Food consumption was measured 1 week prior to initiation and at weekly intervals thereafter.

Urinalysis was performed at a single time point during week 3 on all animals from the 38-day time point study. For urine collection, animals were placed in individual urine collection cages for approximately 16 hours and were supplied with water but not food. Samples were analyzed using the Yellow IRIS (International Remote Imaging Systems, Chatsworth, CA) for quantity, color, appearance, specific gravity, pH, protein, glucose, ketone, blood, nitrite, urobilinogen, leukocytes, erythrocytes, bacteria, epithelial cells, casts, crystals, sodium, potassium, creatine, creatinine, calcium, and chloride. Urine bilirubin was measured with Ictotest-Reagent tablets (Miles Laboratories).

Postmortem Evaluations and Histopathology

Five animals per group were euthanized with carbon dioxide either at 4 or 24 hours after dosing for both the 4.0- and the 15-mg/kg-dosed animals. Animals that received the second 4 mg/kg dose after 7 days were euthanized 24 hours later. Animals that received the third dose were euthanized on day 38.

Blood for hematology and chemistry measurements was collected at terminal necropsies on days 2, 8, and 38. Standard hematology measurements were taken on a Technicon H1 analyzer using laser optics and cytochemical staining and included total leukocyte counts, total erythrocyte counts, hematocrit, hemoglobin, platelet counts, and differential

TABLE 1.—Study design.

Dosage of adriamycin HCl (IP)	Number of rats	Interval between injections	Number of injections (total dose received)	Duration of exposure before euthanasia	Clontech array (no of arrays)
Saline control*	3	—	1 (0)	4 h	ToxII array #7732-1 (3)
4 mg/kg*	3	—	1 (∼1.2 mg)	4 h	ToxII array #7732-1 (3)
15 mg/kg*	3	—	1 (∼4.5 mg)	4 h	ToxII array #7732-1 (3)
Saline control*	3	—	1 (0)	24 h	ToxII array #7732-1 (3)
4 mg/kg*	3	—	1 (∼1.2 mg)	24 h	ToxII array #7732-1 (3)
15 mg/kg*	3	—	1 (∼4.5 mg)	24 h	ToxII array #7732-1 (3)
Saline control**	5	1 week	2 (0)	8 days	ToxII array #7732-1 (3)
4 mg/kg**	5	1 week	2 (∼2.4 mg)	8 days	ToxII array #7732-1 (3)
Saline control***	5	1 week	4 (0)	38 days	Stress array #7735-1 (2) CDNA expression array #7738-1 (2)
4 mg/kg***	5	1 week	4 (∼4.8 mg)	38 days	Stress array #7735-1 (2) CDNA expression array #7738-1 (2)

*A single dose on day 1 at the dose indicated (either 4 or 15 mg/kg) and blood and tissue collection at the time indicated.

**A single 4-mg/kg dose (or 0 mg/kg for controls) on day 1 followed by a second 4-mg/kg dose (or 0 mg/kg for controls) on day 7 and blood and tissue collection collection 24 hours later.

***Weekly dosing of 4 mg/kg (or 0 mg/kg for controls) for a total of 4 doses with dosing being interrupted during week 3 due to the poor condition of the animals.

leukocyte counts (neutrophils, lymphocytes, and monocytes). Reticulocyte counts were performed on a Sysmex R3000, semiautomated reticulocyte analyzer. Routine serum chemistries were performed on a BMC/Hitachi 911 instrument using standard reagents and protocols and included albumin, alkaline phosphatase, alanine aminotransferase (ALT), aspartate aminotransferase (AST), total bilirubin (direct and indirect bilirubin was determined if total bilirubin was $\geq$1.2 mg/dL), blood urea nitrogen, cholesterol, triglycerides, total protein, calcium, glucose, total bile acids, phosphorus, sodium, potassium, chloride, globulin (calculated), and albumin/globulin ratio (calculated) (A/G Ratio). Insulin levels were determined using an ELISA Assay from Mecordia AB, Uppsala, Sweden according to the manufacturer's instructions.

All animals received complete postmortem examinations and the following tissues were collected for histopathologic evaluation: heart, liver, blood, kidney, ileum, colon, cecum, bone marrow (sternum and femur), and gross abnormalities.

Upon removal of the heart and after heart weights were obtained, midventricular transverse sections were taken and fixed in 10% neutral buffered formalin for routine histologic processing, and paraffin embedding and staining with hematoxylin and eosin. The remainder of the heart was snap frozen in liquid nitrogen for Total RNA isolation.

Blood Sample RNA Isolation

Blood samples for gene analysis were collected at 4 and 24 hours and 8 days (24 hours after the second dose) for the 4-mg/kg/wk dose and at 4 hours and 24 hours for the 15-mg/kg dose group. In each case, 2 ml of whole blood were collected directly into 3 ml of Trizol Reagent. Total RNA was isolated by chloroform extraction and isopropanol and ethanol precipitation and samples were suspended in RNase-free water and frozen at -80°C.

Heart Sample RNA Isolation

Snap-frozen hearts were placed directly into Trizol Reagent and homogenized using a Polytron model PCU11. Total RNA was isolated by chloroform extraction and isopropanol and ethanol precipitation and samples were suspended in RNase-free water and frozen at -80°C.

cDNA Array Hybridization

Clontech Rat Toxicology II arrays were used to evaluate differential gene expression for all but the 38-day time point. For the 38-day time point, Clontech Rat Atlas™ cDNA Expression and Stress Arrays were used. Each of these cDNA arrays use plasmid and bacteriophage DNAs as negative controls and have several housekeeping genes as positive controls for normalization, although a global method of normalization was used in this experiment. Details of the gene composition of each of the arrays used can be found at ⟨www.atlasinfo.clontech.com⟩. A brief summary of each array is listed below:

Gene array	Catalog number	Number of genes on the array
Rat Tox II	7732-1	465
Rat Stress	7735-1	207
Rat cDNA expression	7738-1	588

In all cases, total RNA was evaluated for degradation by electrophoresis through a formaldehyde containing 1% agarose gel with ethidium bromide staining prior to use. Five micrograms of total RNA from 3 treated and 3 control hearts and blood samples were used for generating ^{33}P labeled probes by reverse transcription. Probes were hybridized overnight at 62°C using Microhyb buffer (Research Genetics). After stringent washes, filters were placed on a Packard Cyclone Phosphor Image Scanner and scanned images saved as TIFF files. TIFF files were aligned using Clontech Atlas Image 1.5 or 2.0 software.

Statistical Analysis of Gene Arrays

Following global background subtraction by Atlas Image software, adjusted intensities were normalized and statistically evaluated by a custom analysis software program written expressly for gene expression analysis called NLR [Normalization and Local Regression] (4). NLR was used to compare control with treated groups (n = 3/group), generate *p*-values, an indication of signal intensity (MLI, mean log intensity), and ratios of differences between groups. Selected gene expression changes were examined for confirmation of the direction and degree of change using RT-PCR (Taqman) based on the signal intensity and fold changes and on correlation with reported mechanisms of toxicity.

Taqman Real-Time Quantitative RT-PCR

Quantification of mRNA was carried out using Molecular Probes' Ribogreen RNA Quantification kit. To prevent amplification of genomic DNA sequences, all RNA samples were treated with DNase I and diluted to 10 ng/μl. Taqman probes were labeled with FAM (carboxyfluorescein) as the reporter dye on the 5′ position and TAMRA (carboxytetramethylrhodamine) as the quencher dye on the 3′ position. cDNA was made using MMuLV (Moloney Murine Leukemia Virus). All reactions were carried out in a single tube reaction setup on an ABI PRISM 7700 Sequence Detection System (Applied Biosystems, Inc). The following temperature profile was used: 30 minutes at 48°C for RT, 10 minutes at 95°C for RT inactivation and AmpliTaq Gold activation, 40 cycles of 15 seconds at 94°C, and 1 minute at 60°C. To check for possible contamination in the reaction mix, No Template Control (NTC) wells without RNA template were used. The cycle threshold Ct (ie, 10 times the standard deviation of the mean baseline emmision calculated during PCR cycles 3 to 15) was used to calculate relative amounts of target RNA. The delta Ct method was used to calculate relative fold expression levels, as described by Applied Biosystems. Primers and probes were purchased from Keystone Biosource (Camarillo, CA). Final concentrations of all primers were at 900 nM, probes were at 200 nM. Primer sequences are listed in Table 2.

RESULTS

Hematology

The hematologic profiles for the control and treated samples reported here are summarized in Table 3. The hematologic profile comparing the vehicle to the untreated control indicates that the pH of the injectable adriamycin, has very

TABLE 2.—Sequences of the primers and probes.

Gene	Forward primer	Reverse primer	Probe
Cyclin D1	CCCACGATTTCATCGAACACT	TGTGCATGTTTGCGGATGAT	FAM-AAAATGCCAGAGGCGGATGAGAACAA-TAMRA
GADD45	GCTGGCTGCGGATGAAGAT	CACGAATGAGGGTGAAATGGA	FAM-ACGACCGGGACGTGGCTCTGC-TAMRA
GPX	GTGTTCCAGTGCGCAGATACA	GCAGGGCTTCTATATCGGGTT	FAM-CAGGCGCTTTCGCACCATCGAC-TAMRA
HO-1	GAAGGGCTGCCCTAGAGCA	GGATGAGTACCTCCCACCTCG	FAM-CACACCAGCCACACAGCACTACGTAAAGC-TAMRA
HSP70	ACCATCCCCACCAAGCAGA	CCTCGTACACCTGGATCAGCA	FAM-CTTCACCACCTACTCGGACAACCAGCC-TAMRA
PTGS1	TTCCAGTATCGCAACCGCA	AGGAATCAGGCATGAACGGAT	FAM-CGCCATGGAATTCAACCACCTCTATCAC-TAMRA
NMOR	ATCCGCCCCCAACTTCTG	CTCTCTGCGTGGGCCAATAC	FAM-CATGGCGGTGAGAAGAGCCCTGA-TAMRA
MDR1	CCACGATTGCCGAAAACATT	CATTGGCTTCCTTGACAGCTT	FAM-TGGCCGAGAAAACGTCACCATGGAT-TAMRA
WAF1	GTTCCGCACAGGAGCAAAG	CGGCTCAACTGCTCACTGTC	FAM-ATGCCGTCGTCTGTTCGGTCCC-TAMRA

little effect as compared to the variability between animals, at the 4- and 24-hour time points. In general, significant and dose related decreases in lymphocytes were noted at the 4-hour, 24-hour, and 8-day sampling periods, both as a result of the inevitable stress associated with administration of the drug and as a result of its lymphocyotoxic effects. Because lymphocytes make up the most significant fraction of nucleated white blood cells, the drop in lymphocyte number may have influenced what was perceived as a downregulation of many blood genes. Reticulocyte counts tended to be depressed at the 15-mg/kg dose at 24 hours and to decrease with time at the 4-mg/kg dose. There was no effect on hematocrit and no indication of dehydration at the 4- and 24-hour time points, yet a significant decline in hematocrit occurred by day 38. Platelet counts did not fall in response to treatment. There were occasional immediate increases in neutrophils and monocytes in response to the necrotizing effects of ip injection of adriamycin. At the 15-mg/kg dose at 24 hours, there was very little difference in neutrophils and monocytes as compared to the vehicle control.

Clinical Chemistry

Clinical chemistry findings are presented in Table 4. There were few significant changes in the clinical pathology parameters measured at either the 4- or 24-hour sampling points at the 15-mg/kg dose. There were changes in AST at all time points that suggested probable subperitoneal muscle damage at the site of injection (not discussed in this paper but noted by histopathology), but these were not statistically significant. Statistically significant elevations in serum phosphorus at 4 hours may be an indication of the massive intestinal and lymphoid apoptosis at this time. The statistically significant decreases in BUN and elevations in total cholesterol were not considered to be physiologically meaningful.

By day 38, after 3 doses of 4 mg/kg each week, there was clear evidence of adriamycin-induced nephrotic syndrome, with statistically significant decreases in total protein and albumin, and increases in BUN, creatinine, and total cholesterol. Reduced food intake also contributed to hypoglycemia. Based on the clinical chemistry and histology of the kidney at 8 days, the heart and blood gene expression at 4 and 24 hours, and 8 days would not be significantly affected by secondary physiologic alterations resulting from adriamycin-induced kidney lesions, but beyond that, responses might reflect the complexity of the effects of hypoproteinemia, hypercholesterolemia, elevated serum creatinine, and hypoglycemia and dehydration.

Histopathology

Thewell-recognized histopathologic lesions reported following administration of adriamycin to rats were seen in a dose-related fashion in this study. The chronology of morphologic lesions in relation to gene expression in the heart and blood was revealing. Massive numbers of apoptotic bodies occurred in the crypts of the ileum, cecum, and colon at the 4-hour sampling point at the 15-mg/kg dose level (Figure 1) and lymphatic dilatation with swollen endothelial cells could be found. There was also increased lymphoid cell apoptosis

TABLE 3.—Mean white blood cell counts, hematocrit, and platelets at 4 hours, 24 hours, 8 days, and 38 days.

	Mean total WBC (×1000/cmm)	Mean abs neut (cells/cmm)	Mean abs lymph (cells/cmm)	Mean abs mono (cells/cmm)	Mean reticulocyte number $\times 10^9$/L	Mean hematocrit	Platelets (×1000/cmm)
Untreated control-4 hrs (n = 3)	10.74	3,570	6,562	526	219	44.10	795
Untreated control-24 hrs (n = 3)	5.65	754	4,630	146	216	44.83	774
Vehicle control-4 hrs (n = 3)	8.595	1,050	7,140	237.0	231	42.15	865
Vehicle control-24 hrs (n = 3)	8.380	1,320	6,620	262.5	198	44.80	754
Dose $1X^{\Phi}$ 15 mg/kg-4 hrs (n = 3)	7.907	1,600	5,510	702.7	211	43.93	830
Dose 1X 15 mg/kg-24 hrs (n = 3)	7.853	2,560	4,900	274.7	162	44.43	871
Dose 1X 4 mg/kg-4 hrs (n = 3)	8.653	1,290	6,830	362.0	240	42.50	712
Dose 1X 4 mg/kg-24 hrs (n = 3)	9.583	3,370	5,860	254.0	192	45.13	800
Control-8d (n = 5)	4.994	893	3,950	53.0	173	42.1	657
Dose $2X^{\Phi\Phi}$-8d 4 mg/kg (n = 3)	2.716	1,530	1,140*	28.2	61	42.3	1,332
Control-38d (n = 4)	3.708	580	3,020	45.0	158	40.8	681
Dose $4X^{\Phi\Phi\Phi}$-38d 4 mg/kg (n = 3)	2.505	1,840*	516*	130.3	63	26.7	1,300

*Statistically significant at $p < .05$.
Dose $1X^{\Phi}$ = a single dose on day 1 at the dose indicated (either 4 or 15 mg/kg) and blood collection at the time indicated.
Dose $2X^{\Phi\Phi}$ = a single 4 mg/kg dose on day 1 followed by a second 4-mg/kg dose on day 7 and blood collection at the time indicated.
Dose $4X^{\Phi\Phi\Phi}$ = weekly dosing of 4 mg/kg for a total of 4 doses with dosing being interrupted during week 3 due to the poor condition of the animals.

TABLE 4.—Clinical chemistry at 4 hours, 24 hours, 8 days, and 38 days.

	4 hours				24 hours				2nd dose-day 8				Day 38 (3 weekly doses)			
	Veh. cont. N = 3		15 mg/kg N = 3		Veh. cont. N = 3		15 mg/kg N = 3		Veh. cont. N = 5		4 mg/kg N = 5		Veh. cont. N = 5		4 mg/kg N = 4	
	M	SD	M	SD	M	SD	M	SD	M	SD	M	SD	M	SD	M	SD
Alk Phos. (U/L)	147	11	132	41	216	41	167	40	121	33	48**	3	103	27	213	234
BUN (mg/dl)	15	3	16	2	22	1	18*	1	20	3	15**	1	21	3	52**	17
CPK (U/L)	135	27	165	5	132	11	125	18	NA	NA	NA	NA	NA	NA	NA	NA
AST (U/L)	69	4.5	78	7	76	8.0	105	40	99	57	218**	50	92	12	141	81
ALT (U/L)	41	6.8	36	15.5	45	6.4	56	16.6	38	15	33	7	35	3	36	17
K^+ (meq/L)	6.03	1.1	6.5	.312	6.9	.828	5.8	.612	4.9	.64	5.7	.55	5.1	.12	5.8	.68
Na^+ (meq/L)	148	.98	147	1.4	146	1.3	148	.929	142	3	142	1	143	1	145**	.3
Creatinine	.237	.06	.233	.08	.280	.08	.257	.040	.25	.16	.20	.03	.26	.06	.47	.34
Total protein (g/dl)	6.13	.231	6.07	.252	6.47	.306	6.43	.451	6.2	.25	5.4**	.08	6.2	.17	4.1**	.49
Glucose	203.	12.8	207	2.31	222	23	223	22	183	8	171*	8	180	17	137	48
Albumin (g/dl)	4.43	.321	4.50	.200	4.7	.252	4.50	.436	4.0	.22	3.4	.09	4.2	.17	1.8**	.14
Globulin (g/dl)	1.8	.100	1.6	.058	1.80	.100	1.93	.153	2.1	.35	2.0	.05	2.0	.11	2.3	.36
Calcium (mg/dl)	12.1	.231	12.2	0.00	12.4	.153	12.5	.503	10.1	.4	9.6*	.26	9.8	.27	9.2**	.24
Chloride (meq/l)	99.1	.520	99	.252	102	2.14	100	2.2	104	1	105*	1	105	1	109**	1
Phosphorus (mg/100 ml)	9.20	.100	10.8*	.814	9.7	1.14	11.4	.800	6.1	1.3	7.1	.41	4.6	.35	6.3**	.74
Cholesterol (mg/dl)	51.3	12.7	52.3	5.8	51.3	2.08	62*	4.36	62	4	66	11	67	11	195*	103

NA = not available.
* = significant at $p \leq .05$.
** = significant at $p \leq .01$.

(Figure 1) in gut associated lymphoid tissue (GALT). Apoptosis to a lesser degree was present at the 4-mg/kg dose level and was barely detectable at 2 mg/kg. There was also apoptosis of red and white cell precursors in the bone marrow at this same time point. There were no other lesions observed at 4 hours in any of the other organs sampled. By 24 hours, apoptosis had subsided to a great extent. Pockets of cell debris and occasional apoptotic bodies were present but the number of crypts involved and the numbers of cells/crypt with apoptotic bodies was greatly reduced (Figure 1). There was also a great reduction in lymphoid apoptosis in the GALT (Figure 1). The probability that the maximum pro-apoptotic gene expression occurred prior to the 4-hour sampling point may explain the limited pro-apoptotic gene expression in the blood even though lymphoid cell numbers had fallen by 4 hours.

The necrotizing cell death produced by intraperitoneal injection of either 4 or 15 mg/kg adriamycin into the abdomen was evident at 24 hours when histologically examining serosal surfaces. Although very mild in severity, the extent of mesothelial cell death and liver parenchymal cell death immediately beneath the mesothelium was readily seen (Figure 2) albeit with very little inflammatory response. By day 8, after the second dose, necrosis that extended into the subperitoneal muscle could be seen at the injection site and neutrophilic infiltrates were more prominent, indicating that the increased fluid observed in the abdominal cavity and liver induration were not secondary to heart failure, but were due to a developing peritonitis from the IP injections. Fibrin could be seen adhering to Glisson's capsule and the falciform ligament of the liver in combination with subcapsular hepatocellular necrosis and fibroplasia of the capsule (Figure 2). In the bone marrow, a shift to granulocytic precursors was evident and mast cells and eosinophils were more prominent. In the heart at 8 days, there was very little in the way of altered morphology.

By day 38, and after 4 IP doses at 4 mg/kg, there was a marked fibrinous peritonitis in some animals (Figure 2) and in the heart, clear development of the multifocal cardiomyocyte vacuolation (Figure 3) that is the hallmark of adriamycin cardiomyopathy. In the bone marrow, few erythroid and myeloid precursors could be found whereas megakaryocytes were unaffected and mast cells were more numerous (Figure 3). In the kidney there was marked protein leakage and tubular damage (Figure 3), which matched well with the development of nephrotic syndrome as indicated by the accompanying clinical pathology values for serum protein, albumin, and cholesterol. There were no histopathologic changes associated with administration of the saline or vehicle control solutions at any of the time points examined.

Differential Gene Expression-Fold Change from Clontech Rat ToxII Arrays and Clontech Rat Atlas and Stress Arrays

Control. A ranking of the mean local intensities (MLI) of gene expression computed by NLR (4) from the heart and blood from control animals provides an indication of the baseline expression of the most active genes in an unchallenged state. A complete listing of these results can be found in the Appendix at ⟨http://www.toxpath.org/⟩. In the heart, many highly expressed genes as detected on the Clontech Tox II Array, revolved around cardiac energetics (lactate dehydrogenase B, adenine nucleotide translocator I, mitochondrial enoyl-CoA hydratase precursor, very long chain acyl-CoA dehydrogenase precursor, long chain-specific acyl-CoA dehydrogenase precursor, glutamate oxaloacetic transaminase 1, glyceraldehyde 3-phosphate dehydrogenase), protein synthesis (ribosomal protein L13A) protein folding (heat shock 90-kDa protein beta, heat shock cognate 71-kDa protein, heat shock 60-kDa protein) and disposal (polyubiquitin and 17-kDa ubiquitin-conjugating enzyme E2) as well as antioxidants (manganese-containing superoxide dismutase-2 precursor, copper-zinc-containing superoxide dismutase 1 and thioredoxin). This is all as would be expected in a muscular pump intent on maintaining its composite protein parts and its supply of energy when evaluated on a platform heavily weighted toward these processes.

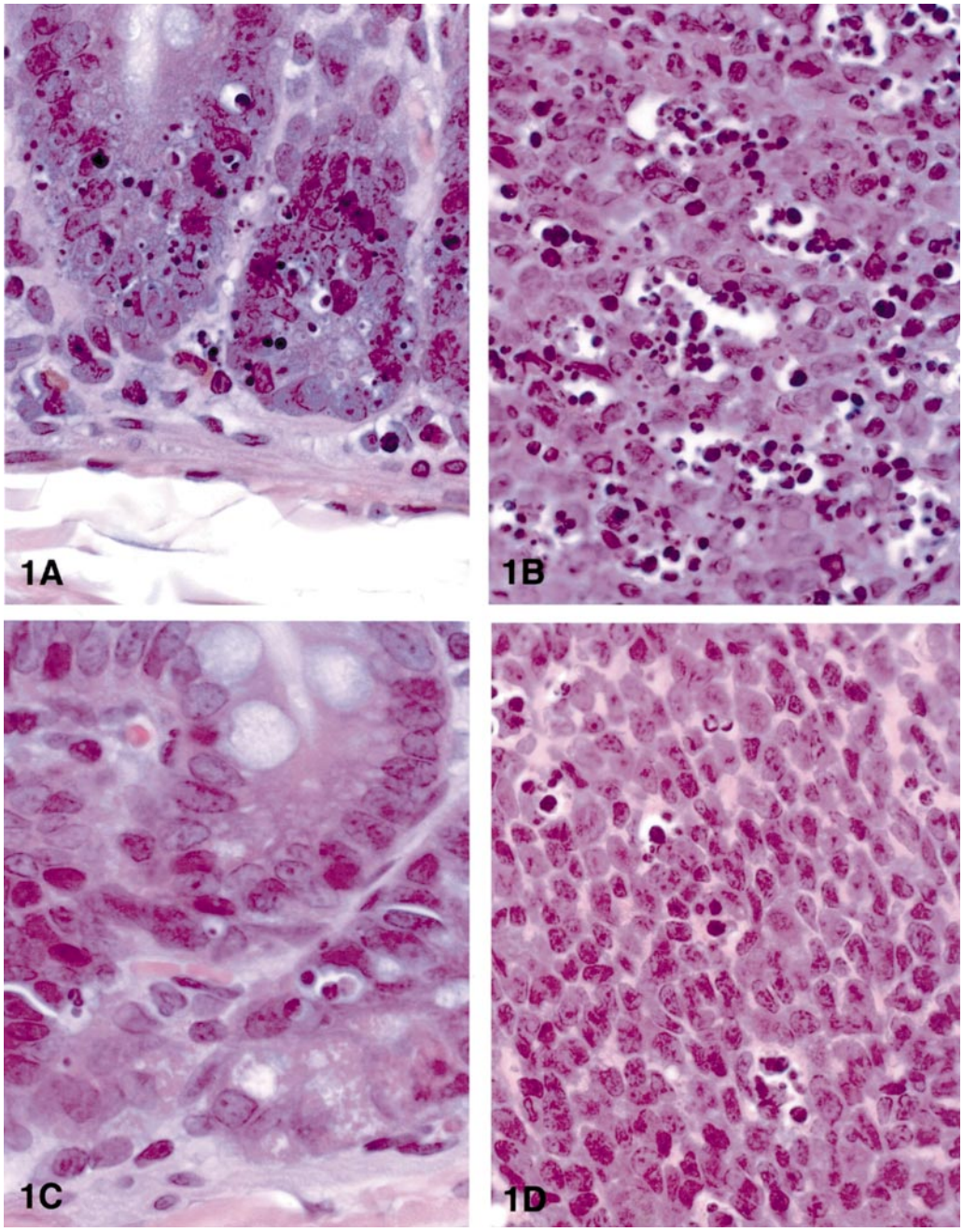

FIGURE 1.—Ileal crypts (A) and gut associated lymphoid tissue (GALT) (B), 4 hours' postadministration of 15 mg/kg adriamycin by IP injection and 24 hours' postadministration (C and D). Note massive numbers of apoptotic bodies in crypts and lymphocytolysis in GALT at 4 hours and their relative absence at 24 hours. Hematoxylin and eosin, ×320.

In the blood, the theme of anti-oxidant protection (liver catalase, thioredoxin peroxidase 1, γ-glutamylcysteine synthetase-regulatory subunit) and protein synthesis (40S ribosomal protein S30, 60S ribosomal protein L6, ribosomal protein S9) could be seen as in the heart but there was also more emphasis on cell differentiation, division, and DNA repair (M-phase inducer phosphatase 2, thymosin beta-10, myeloid cell differentiation protein-1, DNA topoisomerase IIB, and xeroderma pigmentosum group D complementing protein) and inflammatory mediators (arachidonate 12-lipoxygenase and RANTES).

Adriamycin Treated. The differential gene expression observed on the Clontech Tox II Arrays for the 24-hour single dose time point (Table 5) demonstrated a clear dose response when comparing the 4-mg/kg to the 15-mg/kg single dose. There also tended to be excellent correlation of the blood and heart gene expression at this highly toxic dose. The same was not true for the 15-mg/kg dose at the 4-hour time point. Only waf1$^{p21/cip1}$, ID2, and perhaps interleukin-1 receptor antagonist protein precursor had some degree of correlative expression between these tissues at 4 hours. At the 4-mg/kg dose, the same genes that most strongly correlated at

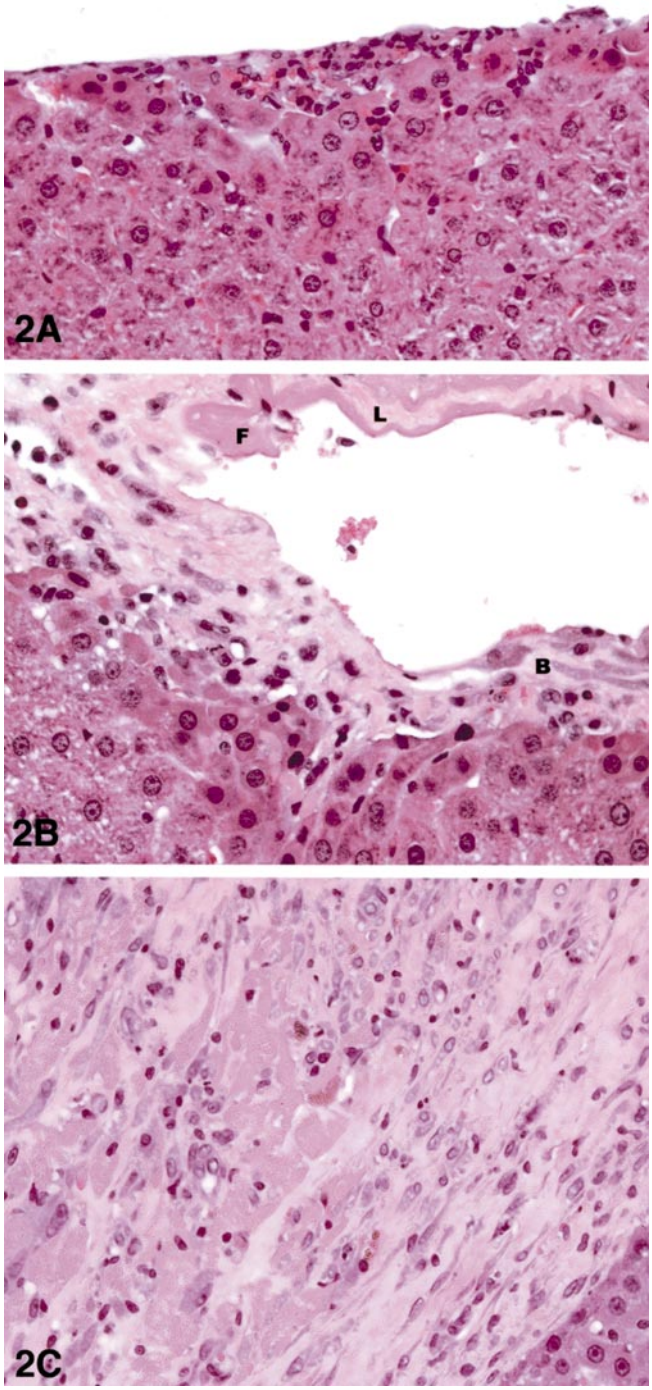

FIGURE 2.—Progression of fibroplasia of Glisson's Capsule with repeated IP injections of adriamycin. (2A) Twenty-four hours after the first 4-mg/kg dose, there is superficial necrosis of the mesothelium and of hepatocytes immediately beneath the capsule with a mild neutrophilic response. (2B) After the second weekly injection (day 8), a layer of fibrin (F) can be seen adherent to the falciform ligament (L) and capsular fibroblasts are prominent (B). (2C) After 4 weekly injections (day 38) there is massive capsular fibroplasia and organization of fibrin. Hematoxylin and eosin, ×400.

15 mg/kg, were not expressed in the heart to the same degree and, with the exception of waf1$^{p21/cip1}$, did not reach statistical significance in both blood and heart. In fact, statistically significant upregulation in the heart was only observed at this dose and time point for glutathione S-transferase Yc1 subunit, Mdr1 and c-erbA-alpha. After 3 weekly doses on day 38, the same upregulation in some of the key stress induced genes such as waf1$^{p21/cip1}$, heme oxygenase 1 (HO-1), and mdr-1 in the heart continued, yet the Ya subunit of glutathione S-transferase which is known to be regulated by oxidative stress was also upregulated. The majority of genes evaluated at this time point were downregulated, however, including c-erb-alpha and NAD(P)H menadione oxidoreductase.

Results of RT-PCR Confirmations

Several total RNA samples from the 4-mg/kg and the 15-mg/kg dose levels at 24 hours were confirmed using real-time quantitative RT-PCR. Examples of these confirmations are presented in Tables 6 and 7, respectively. It is apparent that, although the blood consistently had the most dramatic changes in gene expression and the heart had relatively few, a dose-response occurred reproducibly for several genes, with HO-1 being the most sensitive gene in detecting concurrent changes in blood and heart. The direction of the fold change was very consistently reproduced between the Clontech Arrays and Taqman RT-PCR. There was also usually good agreement between pairs of treated and control heart and blood samples analyzed on the same platform, at least at the 15-mg/kg dose. There did not appear to be consistency between the fold changes when the 2 platforms were compared to each other except in terms of direction of change. This is largely because fold change is not an absolute value but a relative value influenced by background and intensity of radionucleotide incorporation and variables in hybridization between membranes even after normalization. Even so, an appropriate statistical sample and analysis using NLR gives highly reproducible results.

DISCUSSION

Adriamycin is an important component of many chemotherapeutic regimens in the treatment of a variety of cancers including small cell, renal cell, and breast carcinoma. The clinical effectiveness of adriamycin is limited by the dose-dependent cardiotoxicity observed at exposures above 300 mg/m^2. Monitoring the cardiotoxicity of adriamycin has been a critical task since the recognition of the cumulative-dose associated cardiomyopathy. In the past, sequential heart biopsy was the preferred and most reliable method of evaluation (5–7). Elevated plasma levels of endothelin (8) have also been proposed as an indicator of developing adriamycin cardiotoxicity.

Differential gene expression (DGE) by cDNA or oligonucleotide microarrays has proven to be a powerful tool for dissecting patterns of gene expression associated with toxicants. We chose to apply microarray DGE to blood and heart samples in an effort to identify patterns of gene expression that were altered simultaneously in the blood and heart. These genes might then be correlated with the progression of adriamycin toxicity with an eye toward developing blood-based gene expression monitoring. Fortunately a great deal of mechanistic information is available for adriamycin cardiomyopathy. Proposed mechanisms are numerous and interwoven in their effects on: cell signaling (9); cellular energy balance (10–12); cell cycle arrest (9, 13); cellular calcium distribution (14); DNA intercalation, damage, and

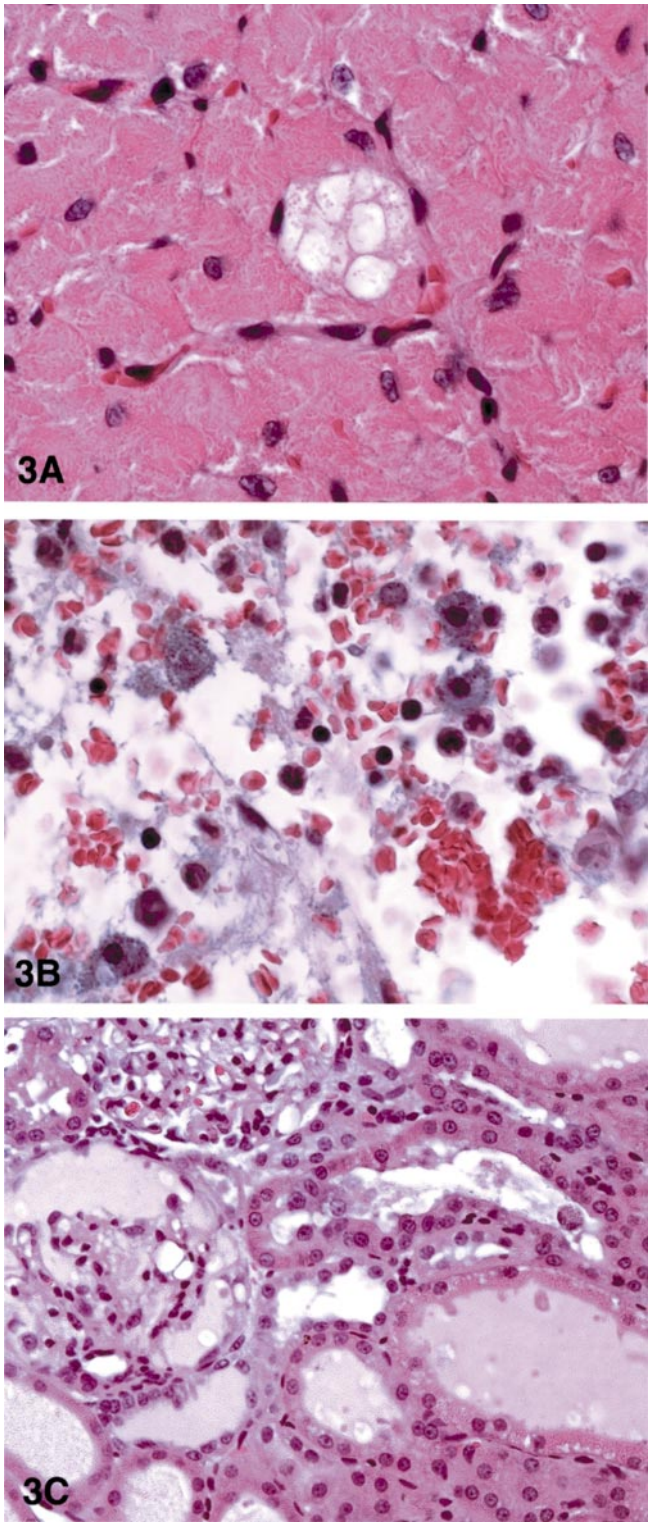

FIGURE 3.—Pathology on day 38 after four 4 mg/kg IP injections of adriamycin. (3A) Heart. Cytoplasmic vacuolar degeneration characteristic of adriamycin-induced cardiomyopathy. Hematoxylin and eosin, ×400. (3B) Femoral bone marrow. Degranulating mast cells, fibrin, and hemorrhage can be seen but virtually no erythroid or myeloid precursors are present. Hematoxylin and eosin, ×480. (3C) Kidney. Characteristic glomerular protein leakage, tubular cell necrosis, and tubular protein casts. Hematoxylin and eosin, ×300.

repair (15); and decreased protein synthesis (16). The quandary of adriamycin-induced cardiac toxicity has always been the delay in onset of clinical and morphologic changes and the clear relationship with cumulative dose.

Oxidative stress has been identified by numerous investigators as a major contributor to the cardiac toxicity induced by adriamycin (17–19) with effects on all of the processes described here. The relationship of anti-oxidant depletion as an explanation for the delayed cardiac toxicity has been explored in numerous animal and cell-based models. Based on single-dose studies in mice, it appears that glutathione is depleted within minutes to hours after dosing, with recovery lagging by only a few hours and largely returning to normal by 24 hours if that dose is not one that overwhelms the system (19, 20). The early response is probably due to enzyme activation of γ-glutamylcysteine synthetase (γGCS), the rate-limiting enzyme in glutathione biosynthesis, which is under the kinetic control of cellular levels of reduced glutathione and cysteine. The delayed response involving transcriptional upregulation of the γ-GCS gene and of other anti-oxidant enzymes such as CuZn-SOD, Mn-SOD, catalase, glutathione peroxidase, and metallothionine may only occur after depletion of protectants or substrates for protectants reach a critical juncture. It has been shown for Mn-SOD in astroglia, that HO-1 must first be upregulated to initiate transcription (21). It has also been shown that for a single overwhelming dose of adriamycin (15 mg/kg) given intraperitoneally, that glutathione levels do not completely recover (20) but that oxidative damage and anti-oxidant gene expression peak on day 4.

The consequences of incomplete protection prior to an adequate response, are multiple molecular defects, albeit functionally this may not be known immediately. By day 4, the translational machinery may be sufficiently damaged to incompletely process the transcripts and indeed, lack of translation in the face of increased transcription has been shown (20). At low doses that cumulatively produce the cardiomyopathy, however, it is not until after 8 weeks of dosing that apoptosis is initiated through a Fas-mediated pathway (22). With loss of cardiomyocytes, the remaining cells would be expected to hypertrophy. Paradoxically we and others saw myocyte atrophy with continued dosing (23). Thus, protein synthesis in cardiomyocytes, which should respond via the Frank-Starling mechanism to enhanced stretch induced demands (24), does not, whereas fibrocytes do respond with increased collagen synthesis and deposition (23).

In designing this study, we reasoned that sequential gene expression in the heart measured at early time points (4 and 24 hours) and followed at a later time point (8 days) until the development of cardiomyopathy (day 38), would provide evidence of the earliest molecular insults. It would also provide evidence of the progression of different downstream mechanisms and of the subsequent events that might delineate when a threshold was crossed that signaled the eventual sequelae of cardiomyopathy. We anticipated that at least some of the transcriptional events in the heart might also be reflected in the blood and that simultaneous sampling of the blood and heart using cDNA arrays may provide a picture of the progression of toxicity in the heart. Ultimately this might allow

TABLE 5.—Gene expression (fold change) in the heart and blood from 3 treated and 3 control animals as calculated by NLR from Clontech arrays or Taqman (where indicated).

Gene	IP dose	4 h–1 dose		24 h–1 dose		Day 8–2 doses 7 days apart		Day 38–4 doses, at weekly intervals heart[€]
		Blood	Heart	Blood	Heart	Blood	Heart	
P21(waf1$^{p21/cip1}$)	4 mg/kg			2.5*	1.46*	2.7*	1.83*	1.98*$^{\phi}$
	15 mg/kg	3.91*	4.48*	11.2*$^{\phi}$	4.82*$^{\phi}$			
NAD(P)H oxido-reductase	4 mg/kg			2.67*	1.22	1.48	1.42	1.5$^{\phi\Phi}$
	15 mg/kg	1.45	1.32	3.59*$^{\phi}$	2.95*$^{\phi}$			
Heme oxygenase I	4 mg/kg			2.31*	1.37	1.31	2.34*	17.6$^{\phi\Phi}$
	15 mg/kg	1.8*	1.04	3.61*$^{\phi}$	2.6*$^{\phi}$			
Mdr1	4 mg/kg			1.07	2.46*	−1.19$^{\Psi}$	4.77*	2.42*$^{\phi}$
	15 mg/kg	−1.02	4.49*	1.8*$^{\phi}$	16.6*$^{\phi}$			
Mdm2	4 mg/kg			1.34	1.07	1.08	1.26	1.11
	15 mg/kg	1.29	−1.07	2.32*	1.83*			
Glutathione S-transferase	4 mg/kg			−1.14	1.41*	2.77*	1.92*	NA
Yc1 subunit	15 mg/kg	−1.04	1.37	1.9*	6.52*			
BTG2	4 mg/kg			1.23	1.19	−1.43	1.03	NA
	15 mg/kg	1.02	2.52*	1.81*	1.52*			
ID2	4 mg/kg			1.53	1.05	1.29	1.05	−1.86*
	15 mg/kg	1.53*	2.38*	1.92*	1.25			
MnSOD	4 mg/kg			2.44*	−1.11	2.99*	1.05	1.1
	15 mg/kg	−1.06	1.17	4.48*	1.15			
iNOS	4 mg/kg			16.5*	1.16	−1.14	1.12	−1.18
	15 mg/kg	1.76*	−2.18*	10.9*	1.28			
Endothelin-converting enzyme	4 mg/kg			2.06*	1.04	1.16	1.18	1.43
	15 mg/kg	1.67*	1.15	1.8*	−1.00			
c-erb-alpha	4 mg/kg			−1.13	1.32	1.32	4.69*	−1.26
	15 mg/kg	−1.05	−1.39	1.47	2.73*			
Microsomal GST	4 mg/kg			2.42	1.31	1.78*	1.73*	1.62
	15 mg/kg	2.59*	−1.23	1.74*	2.69*			
Glutathione S-transferase Ya subunit	4 mg/kg			−1.49	1.17	1.37	1.28	4.25**
	15 mg/kg	−1.09	−1.16	−1.25	3.64*			
Lipopolysaccharide binding protein	4 mg/kg			2.32*	1.29	2.01*	1.9*	NA
	15 mg/kg	2.86*	−1.22	2.7*	1.33			
Interleukin 1 receptor antagonist	4 mg/kg			2.58*	1.69	1.19	1.01	NA
protein precursor	15 mg/kg	1.71*	1.3	4.84*	2.29*			

*Statistically significant at $p < .05$.
**Statistically significant but signal is too low to be reliable (near background).
[€]Blood was not available for evaluation.
NA = Gene cDNA not available on membrane used.
ϕ = Confirmed by RT-PCR at a level near the fold change reported.
Φ = Value based on the average of 2 RT-PCR runs.
Ψ = Downregulated.

monitoring of that progression via blood gene expression in patients. A large number of genes were both up and downregulated in blood and heart by treatment with adriamycin. This discussion will be primarily confined to genes that were upregulated at the 4- and 24-hour time points, due to possible confounding effects of secondary toxicity and declines in the most abundant altered nucleated cell population (lymphocytes) in the blood with continued dosing.

Plotting the gene expression patterns over time and correlating the expression with the hematologic profile and the observed tissue morphology produces a picture that corroborates what is known about adriamycin and suggests additional experiments for both ameliorative procedures and monitoring. Based on transcriptional responses, 4 initiating events were considered probable during the first 4 hours of adriamycin exposure: generation of reactive oxygen species

TABLE 6.—Taqman confirmations vs Clontech Tox II array fold changes for adriamycin at the 15- and 4-mg/kg dose, 24 hours after dosing.

Gene	Pairwise comparison	Fold change at 15 mg/kg				Pairwise comparison	Fold change at 4 mg/kg			
		Taqman result		Clontech array result			Taqman result		Clontech array result	
		Blood	Heart	Blood	Heart		Blood	Heart	Blood	Heart
Cyclin D1	13c v 37t	33457*	3.73	15	1.86	13c v 28t	1.0	−1.03	1.0	1.94
	14c v 38t	23905*	2.3	5**	3.06	14c v 29t	1.0	1.14	1.0	1.04
Gadd45	13c v 37t	2.01	3.15	4.03	2.12	13c v 28t	1.29	1.57	1.63	1.91
	14c v 38t	1.86	2.6	4.45	1.75	14c v 29t	3.07	1.13	2.0	1.56
Heme oxygenase 1	13c v 37t	14.77	55.52	25	4.91	13c v 28t	30.48	4.52	7**	1.64
	14c v 38t	36.63	3.77	6.67	5.38	14c v 29t	68.12	4.23	1.14	1.85
Mdr-1	13c v 37t	3.18	10.16	4**	88	13c v 28t	1.24	1.07	1.0	9.0**
	14c v 38t	4.55	8.06	2	103	14c v 29t	2.25	−1.12	1.0	1.0
NAD(P)H menadione	13c v 37t	10.78	7.92	15.5	5.6	13c v 28t	7.14	1.51	4.25	2.24
oxidoreductase	14c v 38t	3.94	4.29	6	6.5	14c v 29t	4.18	−1.25	3.3	1.32
Waf-1	13c v 37t	3.4	13.59	146	8.34	13c v 28t	−1.02	1.28	4.75	1.77
	14c v 38t	2.08	5.98	49	13.60	14c v 29t	−3.32	1.01	1.1	1.51

*The fold difference on Taqman when a gene is not expressed in the controls yields a number divided by a value very close to 0, which produces an artifact when expressed as a ratio.
**The fold difference in Clontech when the signal in controls was below or at the background threshold consisted of the number of pixels above background in the treated.

by redox cycling of the adriamycin semiquinone; absorption of endotoxin; DNA strand breaks by either DNA intercalation or by damage by reactive oxygen species or reactive nitrogen species; and upregulation of ornithine decarboxylase with subsequent activation of histone acetyltransferase. Each of these will be discussed next in light of their chronology of expression and downstream effects. Charts depicting the proposed gene interactions over the time period of this study and with the dose levels merged, are presented in Figures 4 through 7.

Generation of Reactive Oxygen Species by Redox Cycling of the Adriamycin Semiquinone

Redox cycling by the adriamycin semiquinone is well established as a key generator of electrophilic reactive oxygen species (25–27). Electrophilic reactive oxygen species

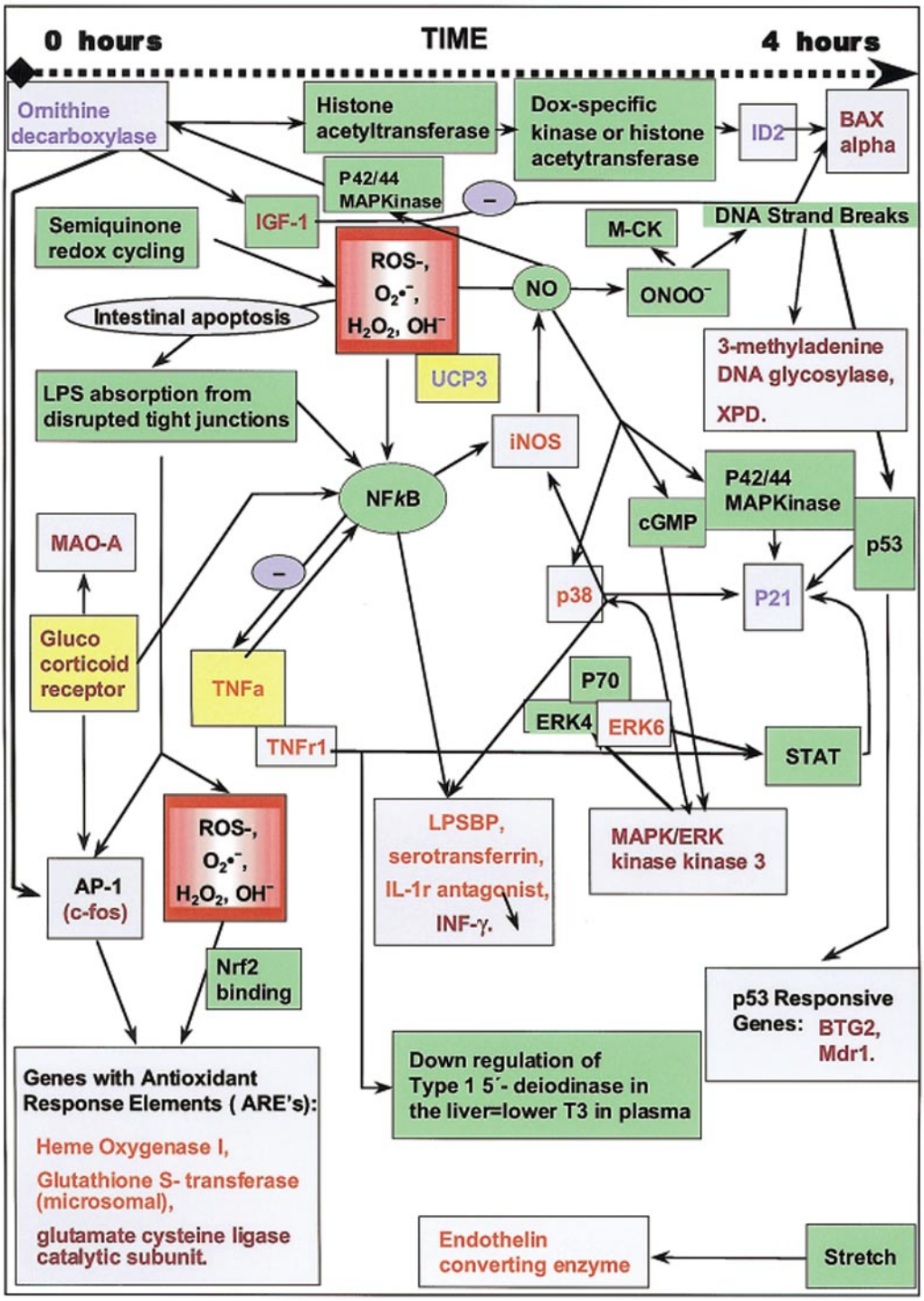

FIGURE 4.—Molecular pathways implicated in the heart and blood during the first 4 hours of high dose adriamycin exposure (see legend for Figure 7).

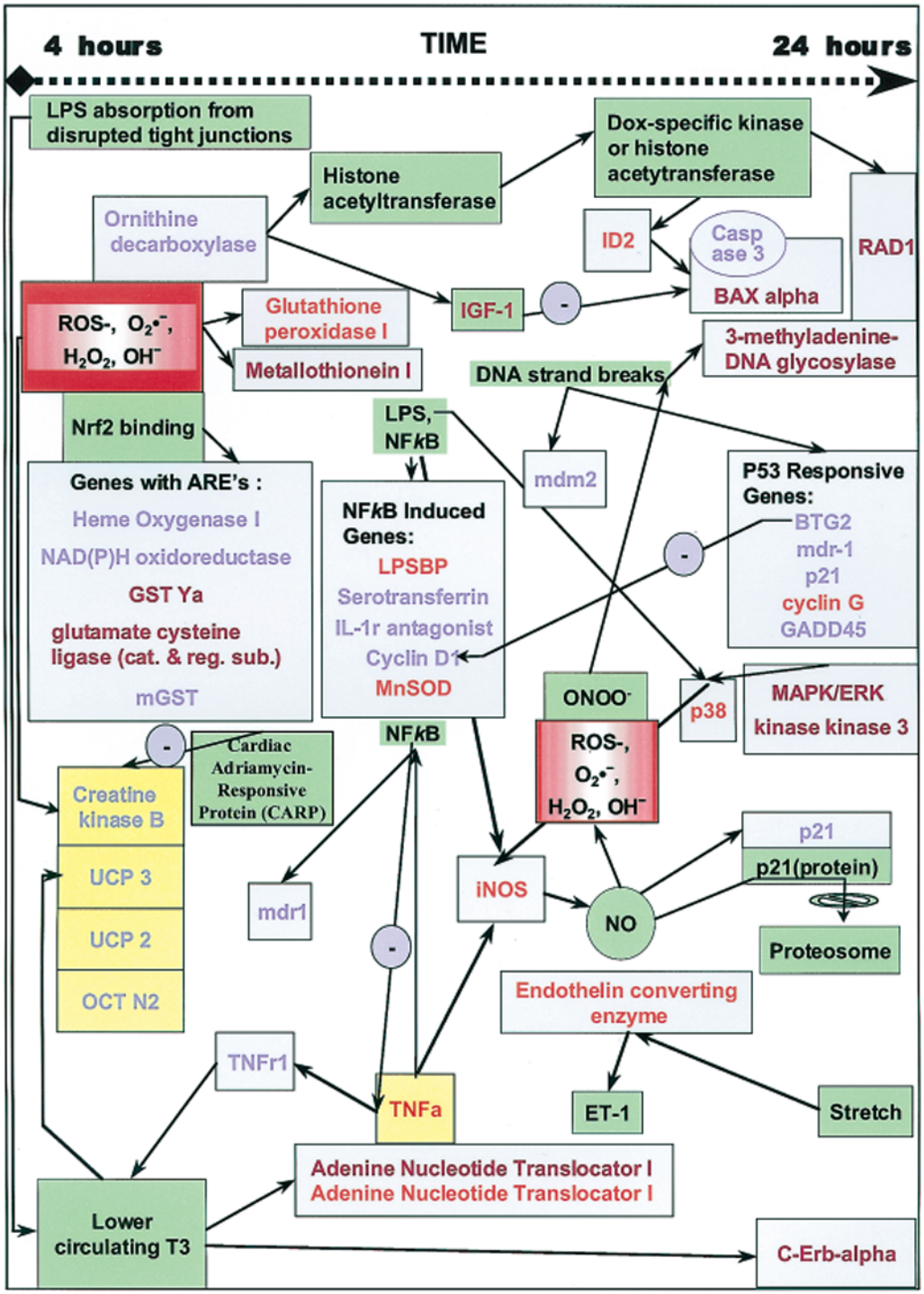

FIGURE 5.—Molecular pathways implicated in the heart and blood from 4 hours to 24 hours after exposure to high dose adriamycin (see legend for Figure 7).

regulate the transcription factor Nrf2 posttranscriptionally. Nrf2, like NF-κB, utilizes an inhibitory protein (Keap1 instead of IκB), and migrates to the nucleus as an active transcription factor only after electrophilic displacement of the inhibitor (28). Downstream targets of the Nrf2 transcription factor includes genes with one or more anti-oxidant response elements (AREs) in their promoter regions. Binding to AREs appears to be additive, providing a mechanism for a graded or positively and negatively controlled response. Several of the genes most consistently upregulated by adriamycin in the first 4 hours contain one or more AREs. These include HO-1,subunits of GST and the γGCS catalytic subunit (29). Their upregulation is essential for cellular protection—HO-1 by preventing hydroxyl radical production via the Fenton reaction; glutathione S-transferases by conjugation of reactive oxygen species with glutathione; and γGCS by controlling

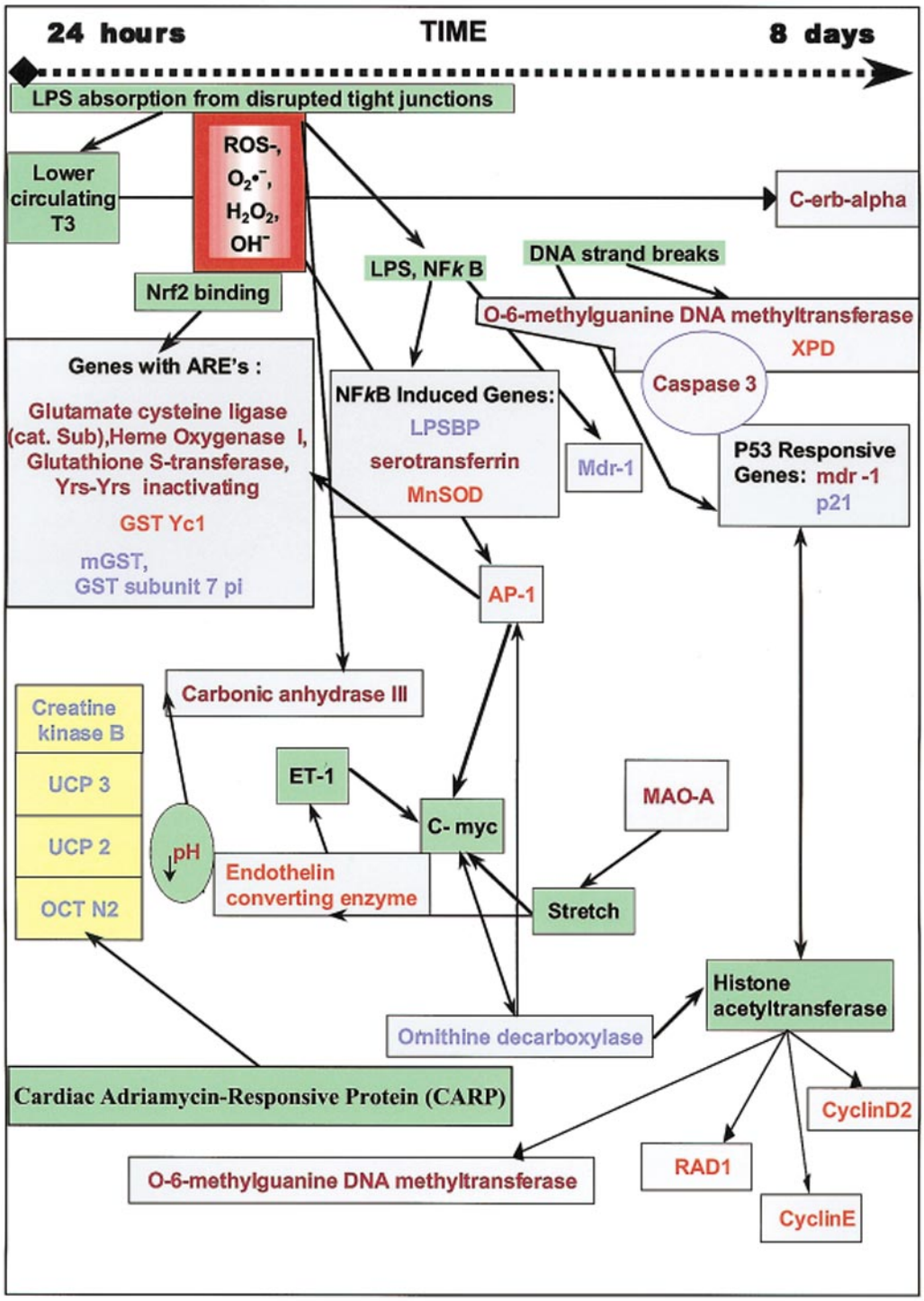

FIGURE 6.—Molecular pathways implicated in the heart and blood after exposure to adriamycin at 4 mg/kg/wk as single injections one week apart. (see legend for Figure 7).

the production of glutathione. It has been shown that the transcription factor Nrf2 activates all of these genes in macrophages in response to oxidative stress (28). Although during the first 4 hours most of the responsive genes were in the blood, γGCS in the heart was upregulated indicating early protective responses to oxidative stress in that organ also.

Absorption of Endotoxin and Activation of NF-κB

During the first 4 hours of adriamycin exposure, in the intestinal tract there is marked apoptosis in the ileal and colonic crypts that may contribute extensively to the subsequent gene expression observed in the heart and blood. Increased permeability of the intestines after adriamycin treatment has

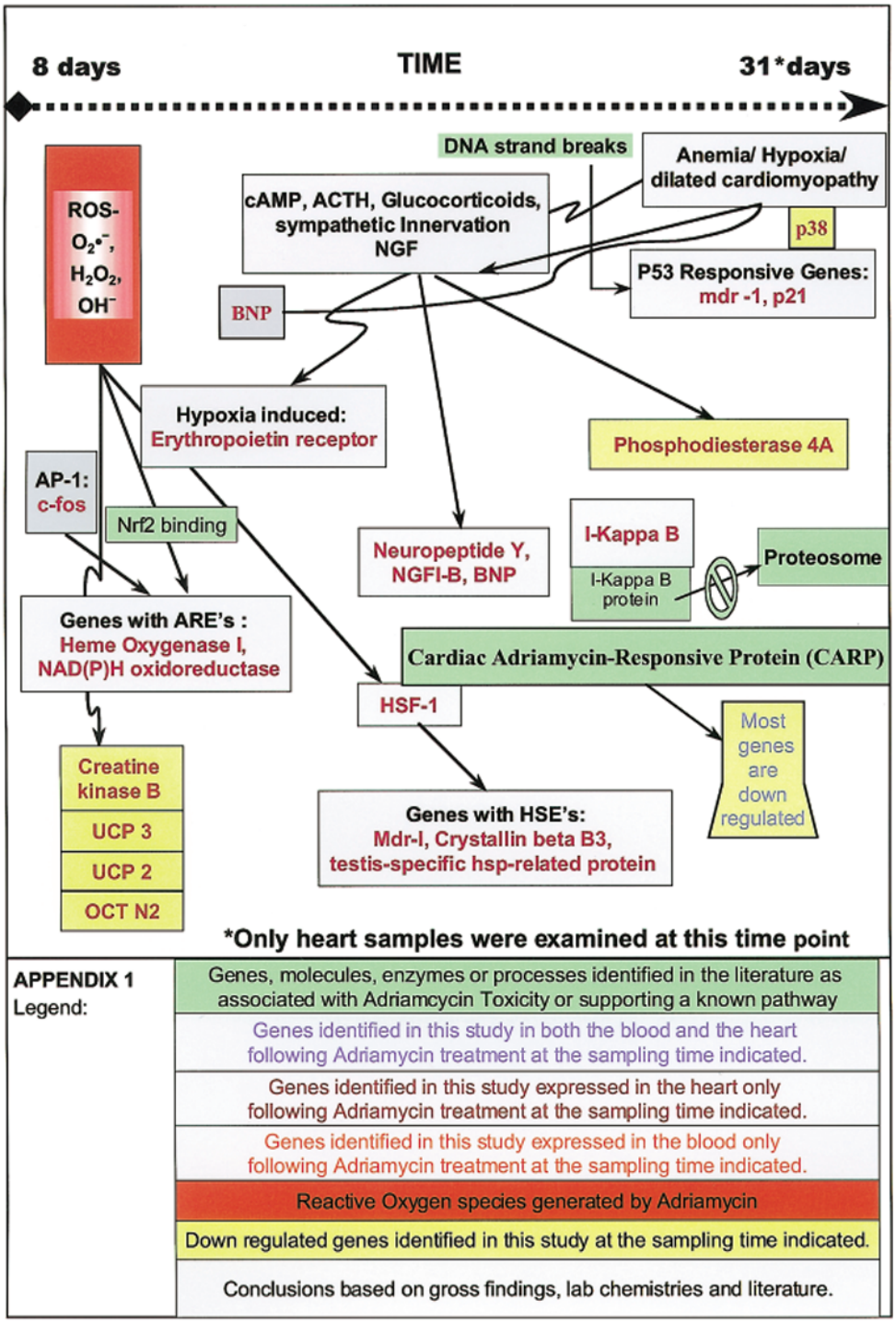

FIGURE 7.—Molecular pathways implicated in the heart after 38 days exposure to adriamycin by 4 weekly injections of adriamycin at 4 mg/kg.

been shown to occur during this time period (30, 31). One pattern of gene expression that we observed during the first 4 hours was very suggestive of endotoxin absorption. Indeed it has been shown that rats receiving high doses of the radiomimetic anti-neoplastics, 5-fluorouracil, or cyclophosphamide had a high incidence of endotoxemia with similar findings reported in human patients (32). Many of the downstream effects of endotoxin are mediated via redox activation of NF-κB (33) from the ERK/STAT signalling pathways (34) or via p38 instead of ERK (35).

A large number of downstream effects of NF-κB seemed to occur in the blood during the first four hours after adriamycin administration. These included upregulation of LPS binding protein (LPSBP), serotransferrin, IL-1 receptor antagonist, and inducible nitric oxide synthase (iNOS). LPSBP is an acute phase protein that can be induced by several cytokines

including IL-1beta, IL-6, and TNF-α. All of these transcripts are induced by endotoxin (36, 37). If endotoxin absorption occurs within the first hour of adriamycin administration, it would be expected that upregulation of LPSBP would occur within the first 4 hours. This is the case for blood at the 15 mg/kg dose. However, induction of LPSBP in the heart does not occur until after the second dose, which either indicates that repeated insults to the intestinal tract increases the absorption of endotoxin or that the upregulation of this protein in the heart is a sensitive indicator of cumulative toxicity that has only reached a critical point and initiated the acute phase response after the second dose. Unfortunately, the level of expression in the blood, although elevated at all time points, does not seem to indicate the timing of the heart upregulation.

TNF-α activates NF-κB, which in turn suppresses apoptosis in ventricular cardiomyocytes (38). Although TNF is known to activate NF-κB and AP1, various studies indicate a peculiarity when adriamycin is co-administered with endotoxin. These reports indicate that adriamycin inhibits or represses the activation of TNF that is normally produced by endotoxin alone (39). The downregulation of TNF-α observed in our study may simply be a counterweight to the numerous NF-κB responses seen after adriamycin administration as a negative feedback loop. In any event, downregulation of TNF-α mRNA in the blood was consistently present in our study while upregulation of the TNF receptor 1 may be a response to the reduction in TNF.

The protein product of the NF-κB-induced gene serotransferrin acts as a sequestering molecule to limit the oxidative availability of iron liberated from heme in the blood by HO-1. It is one of many indicators of the importance of isolating iron from reactive oxygen species as a protective mechanism during oxidative stress.

Interleukin I receptor antagonist (IL-1ra) is the physiologic antagonist of interleukin 1 beta and has anti-inflammatory functions. The gene is also regulated by NF-κB. The upregulation of IL-1ra in the blood in the first 4 hours of treatment may also be a response to absorbed endotoxin. Upregulation of IL-1ra mRNA in the brain following endotoxin administration has been reported and attributed to increased expression from peripherally derived monocytes and macrophages (40). Increased numbers of blood monocytes occur after 4 hours at the 15-mg/kg dose level. Whether this increased number of cells accounts for the apparent increased IL-1ra expression in the blood will need to be pursued further.

Perhaps the most significant downstream effect of NF-κB activation is upregulation of inducible nitric oxide synthase (iNOS) in the blood. It is probable that monocytes account for the majority of this expression. Nitric oxide serves important signaling functions activating MAPK/ERK/p38 and STAT pathways that upregulate $p21^{waf1/cip1}$ and other stress genes, including HSF-1, which initiates mdr-1 transcription, or acts as a pro- or anti-apoptotic mediator in cardiomyocytes (41). Nitric oxide may also increase specific target protein activity by preventing its proteosomal degradation, as for $p21^{waf1/cip1}$ in vascular smooth muscle (42). One of the effects of iNOS induction can be seen in the heart as peroxynitrite formation, the result of NO generation in the presence of reactive oxygen species (43) that has been reported in mice after adriamycin treatment (43).

The resultant damage from the highly reactive peroxynitrite affects a large number of key molecules including the key Kreb's cycle enzyme aconitase (44).

In the case of myofibrillar structure, one of the most heavily nitrated proteins was the myofibrillar isoform of creatine kinase (M-CK) (43). As a key provider of cardiac energy needs, damage to the M-CK protein might be expected to lead to upregulation of the M-CK gene. Unfortunately, the M-CK isozyme was not present on the membranes used in our experiments. The B-CK isozyme was present on the filters, however, and this isoform was significantly downregulated at each time point evaluated. During embryologic development, downregulation of B-CK follows the upregulation of M-CK. This indicates a shift from aerobic to anaerobic respiration. Such a shift would provide a survival advantage in an environment where aerobic metabolism was limited—as would occur due to mitochondrial dysfunction. Reduced mitochondrial creatine kinase activity has been reported following adriamycin administration (45) due to ROS-induced inhibition of the enzyme, and thus such a deficit in aerobic metabolism does appear to be present. The downregulation of UCP3 is also telling as UCP3 expression in the heart may be regulated by the availability of triiodothyronine (T3) (46), which is reduced following adriamycin administration (47), and which should signal reduced aerobic metabolism of fatty acids.

Reactive Oxygen- or Nitrogen-Induced DNA Damage

The other primary consequence of the generation of peroxynitrite is the nitration of DNA, particularly but not exclusively at guanine nucleobases (48), and single strand DNA strandbreaks that led to DNA repair (49). Downstream consequences of this DNA damage is evident in the upregulation of *p*53-responsive genes such as BTG2 and mdr1 as well as DNA excision repair genes 3-methyladenine DNA glycosylase [known to be upregulated by adriamycin and other clastogens (50)] and Xeroderma Pigmentosum Group D complementing protein.

Upregulation of Ornithine Decarboxylase, Increases in Polyamines and Activation of Histone Acetylase

Although upregulation of ornithine decarboxylase (ODC) by adriamycin has previously been reported in a mouse model of skin tumor promotion with 12-O-tetradecanoylphorbol-13-acetate (TPA) (51), upregulation of ODC transcripts in the heart by adriamycin has not been reported, to the best of our knowledge. The significance of ODC regulation of polyamine synthesis and of polyamine levels on cardiac growth and development was first recorded by Casti (52) using a rabbit model of cardiac hypertrophy. The importance of polyamines such as spermine, spermidine, and putrescine, in protein synthesis, stabilization of membranes, and intracellular calcium flux, has recently been addressed by Cohen (53). The importance of polyamines as modulators of histone acetylation and thus gene expression may be their single most important function. The number of genes controlled by polyamine-mediated hyperacetylation has been discussed by Hobbs (54). It has also been shown that ODC in some cell types is upregulated by *p*44/42 mitogen-activated protein kinase (MAPK) (55).

ODC has been shown to be required for upregulation of IGF-1 in a cardiac volume overload model (56) and in TGF-beta mediated cardiac hypertrophy from beta adrenergic stimulation (57). It also upregulates ID2 and BAX-α, both of which are upregulated during the first 4 hours of adriamycin administration. The control of ODC by c-myc provides an autostimulatory loop unless other factors intervene. Thus ODC, by controlling the level of polyamines in the nucleus and the degree of hyperacetylation of histones, alters growth and immediate response genes (c-myc, c-fos, c-jun) (58), regulates the access of other transcription factors to DNA binding sites (ID2), and contributes to apoptotic pathways (BAX-α) and caspase pathways via spermine (59) or prevents the activation of these same pathways (IGF-1). All of these downstream gene effects have been described in various studies with adriamycin and were seen in this study (9, 13, 60–63).

Progression of Gene Expression After the First 4 Hours

The decline in blood concentrations of adriamycin over time are not a reliable indicator of the molecular availability of adriamycin. It has been shown by quantitative microspectrofluorometry that the intranuclear concentration of adriamycin in human leukocytes after a single I.V. bolus injection increased over the first 30 minutes and then did not vary over the next 24 hours even though the plasma volume of the drug decreased (64).

At the 24-hour sampling point, much of the up- and downregulated regulated gene expression seen at 4 hours continued. The major change at this time point was a shift in expression of both ARE-containing genes and NF-κB activated genes away from blood toward more expression by the heart. NAD(P)H oxidoreductase and heme oxygenase were excellent blood markers of ARE cardiac gene changes at 24 hours. The importance of these 2 enzymes as cardiac protectants cannot be overemphasized. NAD(P)H menadione oxidoreductase is expressed at its highest level in the heart in rodents (65). Cardiac anti-oxidants, such as reduced glutathione, glutathione peroxidase, catalase, and superoxide dismutase are usually present at very low levels in the heart (3, 66).

Upregulation of NAD(P)H menadione oxidoreductase has been reported following treatment with electrophiles, including adriamycin (29, 67). This enzyme catalyzes obligate 2 electron transfers that provide protection against the redox cycling that occurs with adriamycin, to produce stable hydroquinones that can be removed by conjugation with glutathione or UDP glucuronic acid. For NAD(P)H oxidoreductase to be effective there must be adequate glutathione and glutathione transferase available for conjugation of the hydroquinone produced. Time course studies, largely reported in mice, show fairly rapid reductions in reduced glutathione levels (GSH) beginning within the first 5 hours after a single dose and extending to 16 hours, followed by recovery in the heart and blood beginning between 12 and 16 hours after dosing (19). At 24 hours, the levels of GSH are reportedly normal. Without NAD(P)H menadione oxidoreductase activity, the anthracycline quinone undergoes a single electron transfer to form a semiquinone that then transfers the electron to superoxide that dismutates to hydrogen peroxide. Unless there is an oxidant-induced increase in intracellular ferritin, hydroxyl radicals are generated by Fenton chemistry, which then react with DNA, proteins, and lipids to form a variety of adducts that alter essential cell functions. Thus, NAD(P)H menadione oxidoreductase is a key detoxifying enzyme for anthracycline quinones and its upregulation is an essential protectant against oxidative damage.

Heme oxygenase 1, an acute phase protein, contains 5 ARE elements (68, 69). It is known to be induced by oxidative stress and to serve 2 important anti-oxidant functions—formation of the antioxidant bilirubin and removal of the pro-oxidant heme to release iron and carbon monoxide (70). Degradation of heme proteins may also expose cells to increased risk from available iron via Fenton chemistry. The increase in intracellular ferritin induced by either HO-1 (71) or via a direct response of the ferritin gene through an ARE in the promoter region (72) effectively sequesters free iron. Also, the coordinated regulation of the genes for HO-1 and ubiquitin has been reported in a porcine model of ischemia and reperfusion in the heart that would link degradation of protein and generation of by-products of heme metabolism, perhaps under the same transciptional controls. Heme oxygenase-2, which is also responsible for iron turnover during oxidant stress typically, is not upregulated.

At 24 hours, the oxidative stress signaling pathways, or at least the heart response to the signaling, clearly had increased, suggesting that oxidative stress in the heart or at least the response to oxidative stress was elevated compared to the 4-hour time point, even with upregulation of protective genes at the earlier time point. There was also more cumulative transcriptional evidence of DNA damage and p53 responsive genes being upregulated in the heart. Again at this time point, upregulation by ornithine decarboxylase was prominent in both the blood and heart; downsteam gene effectors of histone acetylation were particularly prominent in the heart. Increased evidence of apoptosis (BAX-α and caspase 3) or prevention of activation of these same pathways (IGF-1) may have signalled an increase in programmed cell death, with time and continued dosing, under the influence of upregulated ODC expression (58).

There were also some new genes being downregulated in the heart and blood, particularly in the area of energy handling that may have signaled the progression of an energy deficit that began at 4 hours and would continue through the remainder of the study. Downregulated genes included creatine kinase B and UCP3 as previously discussed, but also UCP2 and the carnitine transporter OCT N2. The significance of the latter downregulation may be in the loss of the ability of the heart to transport carnitine necessary for the mitochondrial entry and metabolism of long chain fatty acids, a primary energy source for the heart. At high-dose levels, another gene indicator of altered energetics in the heart and blood—adenine nucleotide translocator I (ANT1)—was upregulated at 24 hours. Upregulation of this gene is particularly pertinent in the heart due to reports of upregulation of this isoform in hearts progressing to dilated cardiomyopathy (73). Although the level of induction in the blood was relatively low (1.62-fold) and slightly missed statistical significance ($p = .066$), if the sensitivity of detection in the blood can be improved, then ANT1 might also serve as a reliable indicator of the onset of dilated cardiomyopathy secondary to adriamycin treatment.

The upregulation of rev-erb alpha (designated c-erb on the Clontech ToxII array) seems to provide a wonderful example of the circuitous effects of adriamycin on gene expression in the heart. Adriamycin lowers circulating T3 (74). The exact mechanism by which this occurs has not been established but in line with our previous observation of probable absorption of endotoxin, we believe it is by downregulating 1,5′deiodinase in the heart and liver, which converts T4 to T3 (75). T3 represses expression of c-erb α in the heart. Rev-erb alpha is transcribed from the opposite strand of the c-erb alpha gene and is a transcriptional repressor. We reason, therefore, that the downregulation of T3 by endotoxin may well be the cause of the upregulation of rev-erb α in the heart and repression of c-erb alpha.

Overall, the 24-hour gene expression pattern, particularly at the highest dose level, indicated even with anti-oxidant genes being upregulated, a progression toward bioenergetic failure, increased apoptosis and dilated cardiomyopathy even though there was no morphologic or functional evidence to this effect at this time.

At 8 days, there was continued expression of ARE responsive genes, especially in the heart and of NF-κB activated genes in both the heart and blood. Functionally, protection against oxidative stress, sequestration of iron and DNA repair were again indicated by the genes in these categories.

The gene expression at 38 days in the heart largely indicated downregulation of most gene expression and differed from that seen at the earlier time points in that a functional worsening seemed to be indicated. Selective inhibition of cardiac muscle gene expression by adriamycin has previously been reported (76). The clinical condition of the animals had deteriorated, food intake was reduced; grossly and histologically, all animals had some evidence of dilated cardiomyopathy. Increases in BNP, neuropeptide Y, and NGFI-B receptor and decreases in phosphodiesterase 4A all indicate volumetric distension and poor outflow accompanied by a compensatory rapid poorly functional rate of contraction and efforts to maximize inotropic activity. There was also an increase in I-$\kappa\beta$ transcripts due to the probable increased proteosomal destruction of I-$\kappa\beta$ protein and the feedback stimulation of I-$\kappa\beta$ transcription. Upregulation of some ARE-responsive genes also continued.

Limitations of this Experiment and of Whole Blood Gene Expression

The direct cytotoxicity of adriamycin is well known. Intraperitoneal injection results in some limited local tissue damage (see histopathology), which probably acts as a stimulus for endogenous corticosteroid and catecholamine release. The changes in cellular composition in the blood and in the tissues due to inflammation appears to be mild at the 4 hour time point, and more apparent at the 24-hour time point. It is not clear to what extent that these limited alterations in cell counts and endogenous stress responses modify the gene expression. We are currently evaluating different techniques for blood collection and separation to answer the cell count issue. Other confounding factors that result from the toxicity of adriamycin and that further alter gene expression include reductions in food intake and renal damage that eventually results in nephrotic syndrome. Because this is not a significant factor at the 4- and 24-hour time points, the early gene expression appears to be the most informative. This study exemplifies the need for pathologic correlation and contextual interpretation of gene expression studies.

SUMMARY

The goal of using blood gene expression to monitor oxidative stress in target organs seems to hold some promise, particularly at high-dose levels. Further studies will be needed to established the boundaries of this correlation and clearer associations of levels of gene expression or gene product with cumulative dose and the development of cardiomyopathy. Detailed time course studies will also be necessary to more completely understand the sequence of gene expression as correlated with morphologic and biochemical changes. With time and the addition of further and perhaps more sensitive gene detection arrays, low-dose effects may become easier to detect. It would seem that even with the limited data available that monitoring of blood gene expression of NAD(P)H menadione oxidoreductase, ornithine decarboxylase, ANT1 and $p21^{waf1/cip1}$ in relation to clinical outcome, might lead to predictive parameters for the dose regulation of adriamycin and perhaps other oxidative stressors. Therapies that target correction of these limiting gene responses might be useful in ameliorating the toxic effects of the drug, hopefully without altering its chemotherapeutic value. A therapeutic approach aimed at reducing the effects of endotoxin on the cardiovascular system in the first few hours after adriamycin administration seems particularly promising as a prophylactic against early cardiac damage.

ACKNOWLEDGMENTS

We appreciate the assistance received from many people, with special thanks to Dirk Sprenger, Betty Gaskill, and Leigh Brown.

REFERENCES

1. Khetawat G, Faraday N, Nealen ML, Vijayan KV, Bolton E, Noga SJ, Bray PF (2000). Human megakaryocytes and platelets contain the estrogen receptor beta and androgen receptor (AR): Testosterone regulates AR expression. *Blood* 95: 2289–2296.
2. Brugnara C (2000). Reticulocyte cellular indices: A new approach in the diagnosis of anemias and monitoring of erythropoietic function. *Crit Rev Clin Lab Sci* 37: 93–130.
3. Doroshow JH, Locker GY, Myers CE (1980). Enzymatic defenses of the mouse heart against reactive oxygen metabolites. *J Clin Invest* 65: 128–135.
4. Crosby LM, Hyder KS, DeAngelo AB, Kepler TB, Gaskill B, Benavides GR, Yoon L, Morgan KT (2000). Morphologic analysis correlates with gene expression changes in cultured F344 rat mesothelial cells. *Toxicol Appl Pharmacol* 169: 205–221.
5. Billingham ME, Mason JW, Bristow MR, Daniels JR (1978). Anthracycline cardiomyopathy monitered by morphologic changes. *Cancer Treat Rep* 62: 865–872.
6. Rowan RA, Masek MA, Billingham ME (1988). Ultrastructural morphometric analysis of endomyocardial biopsies. *Am J Cardiovasc Pathol* 2: 137–144.
7. Bristow MR (1978). Early anthracycline cardiotoxicity. *Am J Med* 65: 823–832.
8. Yamashita J, Ogawa M, Shirakusa T (1995). Plasma endothelin-1 as a marker for doxorubicin cardiotoxicity. *Int J Cancer* 62: 542–547.
9. Kang YJ, Zhou ZX, Wang GW, Buridi A, Klein JB (2000). Suppression by Metallothionein of Doxorubicin-induced cardiomyocyte apoptosis through

inhibition of p38 miton-activated protein kinases. *J Biol Chem* 275: 13690–13698.
10. Yen HC, Oberley TD, Vichitbandha S, Ho YS, St Clair DK (1996). The protective role of manganese superoxide dismutase against adriamycin-induced acute cardiac toxicity in transgenic mice. *J Clin Invest* 98: 1253–1260.
11. Sayed-Ahmed MM, Shaaraway S, Shouman SA, Osman AM (1999). Reversal of doxorubicin-induced cardiac metabolic damage by L-carnitine. *Pharmacol Res* 39: 289–295.
12. Abdel-aleem S, el-Merzabani MM, Sayed-Ahmed M, Taylor DA, Lowe JE (1997). Acute and chronic effects of adriamycin on fatty acid oxidation in isolated cardiac myocytes. *J Mol Cell Cardiol* 29: 789–797.
13. Andrieu-Abadie N, Jaffrezou JP, Hatem S, Laurent G, Levade T, Mercaider JJ (1999). L-carnitine prevents doxorubicin-induced apoptosis of cardiac myocytes: Role of inhibition of ceramide generation. *FASEB J* 13: 1501–1510.
14. Kapelko VI, Williams CP, Gutstein DE, Morgan JP (1996). Abnormal myocardial calcium handling in the early stage of adriamycin cardiomyopathy. *Arch Physiol Biochem* 104: 185–191.
15. Boucek RJJ, Miracle A, Anderson M, Engelman R, Atkinson J, Dodd DA (1999). Persistant effects of doxorubicin on cardiac gene expression. *J Mol Cell Cardiol* 31: 1435–1446.
16. Sazuka Y, Tanizawa H, Takino Y (1989). Effect of adriamycin on DNA, RNA and protein biosyntheses in mouse tissues, in connection with its cardiotoxicity. *Jpn J Cancer Res* 80: 1000–1005.
17. Arnaiz SL, Llesuy S (1993). Oxidative stress in mouse heart by antitumoral drugs: A comparative study of doxorubicin and mitoxantrone. *Toxicology* 77: 31–38.
18. Crescimanno M, Flandina C, Rausa L, Sanguedolce R, D'Alessandro N (1988). Morphological changes and catalase activity in the hearts of CD 1 mice following acute starvation or single doses of doxorubicin, epirubicin or mitoxantrone. *Chemioterapia* 7: 53–59.
19. D'Alessandro N, Rausa L, Crescimanno M (1988). In vivo effects of doxorubicin and isoproterenol on reduced glutathione and H_2O_2 production in mouse heart. *Res Comm Chem Pathol Pharmacol* 62: 19–30.
20. Yin X, Wu H, Chen Y, Kang YJ (1998). Induction of antioxidants by adriamycin in mouse heart. *Biochem Pharmacol* 56: 87–93.
21. Frankel D, Mehindate K, Schipper HM (2000). Role of heme oxygenase-1 in the regulation of manganese superoxide dismutase gene expression in oxidatively-challenged astroglia. *J Cell Physiol* 185: 80–86.
22. Nakamura T, Ueda Y, Juan Y, Katsuda S, Takahashi H, Koh E (2000). Fas-mediated apoptosis in adriamycin-induced cardiomyopathy in rats: In vivo study. *Circulation* 102: 572–578.
23. Toyoda Y, Okada M, Kashem MA (1998). A canine model of dilated cardiomyopathy induced by repetitive intracoronary doxorubicin administration. *J Thor Cardiovasc Surg* 115: 1367–1373.
24. Ruwhof C, van der Laarse A (2000). Mechanical stress-induced cardiac hypertrophy: Mechanisms and signal transduction pathways. *Cardiovasc Res* 47: 23–37.
25. Pinkus R, Weiner LM, Daniel V (1995). Role of quinone-mediated generation of hydroxyl radical in the induction of glutathione S-transferase gene expression. *Biochemistry* 34: 81–88.
26. Jeyaseelan R, Poizat C, Wu HY, Kedes L (1997). Molecular mechanisms of doxorubicin-induced cardiomyopathy. *J Biol Chem* 272: 5828–5832.
27. Gewirtz DA (1999). A critical evaluation of the mechanisms of action proposed for the antitumor effects of the anthracycline antibiotics adriamycin and dauorubicin. *Biochem Pharmacol* 57: 727–741.
28. Ishii T, Itoh K, Takahashi S, Sato H, Yanagawa T, Katoh Y, Bannai S, Yamamoto M (2000). Transcription factor Nrf2 coordinately regulates a group of oxidative stress-inducible genes in macrophages. *J Biol Chem* 275: 16023–16029.
29. Dhakshinamoorthy S, Long DJ 2nd, Jaiswal AK (2000). Antioxidant regulation of genes encoding enzymes that detoxify xenobiotics and carcinogens. *Curr Top Cell Regul* 36: 201–216.
30. Parrilli G, Iaffaioli RV, Martorano M, Cuomo R, Tafuto S, Zampino MG, Budillon G, Bianco AR (1989). Effects of anthracycline therapy on intestinal absorption in patients with advanced breast cancer. *Cancer Res* 49: 3689–3691.
31. Sun Z, Wang X, Wallen R, Deng X, Du X, Hallberg E, Andersson R (1998). The influence of apoptosis on intestinal barrier integrity in rats. *Scand J Gastroenterol* 33: 415–422.
32. Okubo S, Yasunaga K (1983). Clinical and experimental studies on DIC found in carcinoma; correlation between anti-cancer drug administration and endotoxemia. *Jpn J Cancer Clin* 29: 803–806.
33. Janssen-Heininger YMW, Poynter ME, Baeuerle PA (2000). Recent advances towards understanding redox mechanisms in the activation of nuclear factor $\kappa\beta$. *Free Radic Biol Med* 28: 1317–1327.
34. Cowan DB, Poutias DN, Del Nido PJ, McGowan FXJ (2000). CD14-independent activation of cardiomyocyte signal transduction by bacterial endotoxin. *Am J Physiol Heart Circ Physiol* 279: H619–629.
35. Chen CC, Wang JK (1999). p38 but not p44/42 mitogen-activated protein kinase is required for nitric oxide synthase induction mediated by lipopolysaccharide in RAW 264.7 macrophages. *Mol Pharmacol* 55: 481–488.
36. Chen G, McCuskey RS, Reichlin S (2000). Blood interleukin-6 and tumor necrosis factor-alpha elevation after intracerebroventricular injection of *Escherichia coli* endotoxin in the rat is determined by two opposing factors: Peripheral induction by LPS transferred from brain to blood and inhibition of peripheral response by a brain-mediated mechanism. *Neuroimmunomodulation* 8: 59–69.
37. Matsumoto T, Tateda K, Miyazaki S, Furuya N, Ohno A, Ishii Y, Hirakata Y, Yamaguchi K (1999). Fosfomycin alters lipopolysaccharide-induced inflammatory cytokine production in mice. *Antimicrob Agents Chemother* 43: 697–698.
38. Mustapha S, Kirshner A, De Moissac D, Kirshenbaum LA (2000). A direct requirement of nuclear factor-$\kappa\beta$ for suppression of apoptosis in ventricular myocytes. *Am J Physiol Heart Circ Physiol* 279: H939–H945.
39. Pogrebniak HW, Matthews W, Pass HI (1991). Chemotherapy amplifies production of tumor necrosis factor. *Surgery* 110: 231–237.
40. Eriksson C, Nobel S, Winblad B, Schultzberg M (2000). Expression of interleukin 1 alpha and beta, and interleukin 1 receptor antagonist mRNA in the rat central nervous system after peripheral administration of lipopolysaccharides. *Cytokine* 12: 423–431.
41. Stefanelli C, Pignatti C, Tantini B, Stanic I, Bonavita F, Muscari C, Guarnieri C, Clo C, Caldarera CM (1999). Nitric oxide can function as either a killer molecule or an antiapoptotic effector in cardiomyocytes. *Biochim Biophys Acta* 1450: 406–413.
42. Kibbe MR, Li J, Nie S, Watkins SC, Lizonova A, Kovesdi I, Simmons RL, Billiar TR, Tzeng E (2000). Inducible nitric oxide synthase (iNOS) expression upregulates p21 and inhibits vascular smooth muscle cell proliferation through p42/44 mitogen-activated protein kinase activation and independent of *p*53 and cyclic guanosine monophosphate. *J Vasc Surg* 31: 1214–1228.
43. Weinstein DM, Mihm MJ, Bauer JA (2000). Cardiac peroxynitrite formation and left ventricular dysfunction following doxorubicin treatment in mice. *J Pharmacol Exp Ther* 294: 396–401.
44. Tabrizi SJ, Schapira AH (1999). Secondary abnormalities of mitochondrial DNA associated with neurodegeneration. *Biochem Soc Symp* 66: 99–110.
45. Yen HC, Oberley TD, Gairola CG, Szweda LI, St Clair DK (1999). Manganese superoxide dismutase protects mitochondrial complex I against adriamycin-induced cardiomyopathy in transgenic mice. *Arch Biochem Biophys* 362: 59–66.
46. Nagase I, Yoshida S, Canas X, Irie Y, Kimura K, Yoshida T, Saito M (1999). Up-regulation of uncoupling protein 3 by thyroid hormone, peroxisome proliferator-activated receptor ligands and 9-cis retinoic acid in L6 myotubes. *FEBS Lett* 461: 319–322.
47. Valdes Olmos RA, tBHWW, ten Hoeve RF, van Tinteren H, Bruning PF, van Vlies B, Hoefnagel CA (1995). Assessment of anthracycline-related myocardial adrenergic derangement by metaiodobenzylguanidine scintigraphy. *Eur J Cancer* 31A: 26–31.
48. Tretyakova NY, Wishnok JS, Tannenbaum SR (2000). Peroxynitrite-induced secondary oxidative lesions at guanine nucleobases: Chemical stability and recognition by the Fpg DNA repair enzyme. *Chem. Res. Toxicol.* 13: 658–664.

49. Tretyakova NY, Burney S, Pamir B, Wishnok JS, Dedon PC, Wogan GN, Tannenbaum SR (2000). Peroxynitrite-induced DNA damage in the supF gene: Correlation with the mutational spectrum. *Mutat Res* 447: 287–303.
50. Codegoni AM, Broggini M, Pitelli MR, Pantarotto M, Torri V, Mangioni C, D'Incalci M (1997). Expression of genes of potential importance in the response to chemotherapy and DNA repair in patients with ovarian cancer. *Gynecol Oncol* 65: 130–137.
51. Satyamoorthy K, Perchellet JP (1989). Modulation by adriamycin, daunomycin, verapamil, and trifluoperazine of the biochemical processes linked to mouse skin tumor promotion by 12-O-tetradecanoylphorbol-13-acetate. *Cancer Res* 49: 5364–5370.
52. Casti A, Guarnieri C, Dall'asta R, Clo C (1977). Effect of spermine on acetylation of histones in the rabbit heart. *J Mol Cell Cardiol* 9: 63–71.
53. Cohen SC (1998). *A Guide To The Polyamines.* Oxford University Press, New York.
54. Hobbs CA, Gilmour SK (2000). High levels of intracellular polyamines promote histone acetyltransferase activity resulting in chromatin hyperacetylation. *J Cell Biochem* 77: 345–360.
55. Flamigni F, Facchini A, Capanni C, Stefanelli C, Tantini B, Caldarera CM (1999). p44/42 mitogen-activated protein kinase is involved in the expression of ornithine decarboxylase in leukaemia L1210 cells. *Biochem J* 341: 363–369.
56. Friberg P, Isgaard J, Wahlander A, Wickman A, Adams MA (1998). Inhibited expression of insulin-like growth factor I mRNA and attenuated cardiac hypertrophy in volume overloaded hearts treated with difluoromethylornithine. *Growth Horm IGF Res* 8: 159–165.
57. Schluter KD, Frischkopf K, Flesch M, Rosenkranz S, Taimor G, Piper HM (2000). Central role for ornithine decarboxylase in beta-adrenoceptor mediated hypertrophy. *Cardiovasc Res* 45: 410–417.
58. Wang GW, Kang YJ (1998). Inhibition of doxorubicin toxicity in cultured neonatal mouse cardiomyocytes with elevated metallothionein levels. *J Pharmacol Exp Ther* 288: 938–944.
59. Stefanelli C, Stanic I, Zini M, Bonavita F, Flamigni F, Zambonin L, Landi L, Pignatti C, Guarnieri C, Caldarera CM (2000). Polyamines directly induce release of cytochrome *c* from heart mitochondria. *Biochem J* 347: 875–880.
60. Kurabayashi M, Dutta S, Jeyaseelan R, Kedes L (1995). Doxorubicin-induced Id2A gene transcription is targeted at an activating transcription factor/cyclic AMP response element motif through novel mechanisms involving protein kinases distinct from protein kinase C and protein kinase A. *Mol Cell Biol* 15: 6386–6397.
61. Jeyaseelan R, Poizat C, Baker RK, Abdishoo S, Isterabadi LB, Lyons GE, Kedes L (1997). A novel cardiac-restricted target for doxorubicin. *J Biol Chem* 272: 22800–22808.
62. Wang L, Ma W, Markovich R, Lee WL, Wang PH (1998). Insulin-like growth-factor I modulates induction of apoptotic signaling in H9c2 cardiac muscle cells. *Endocrinology* 139: 1354–1360.
63. Kumar D, Kirshenbaum L, Li T, Danelisen I, Singal P (1999). Apoptosis in isolated adult cardiomyocytes exposed to adriamycin. *Ann NY Acad Sci* 874: 156–168.
64. Morjani H, Pignon B, Millot JM, Debal V, Lamiable D, Potron G, Etienne JC, Manfait M (1992). Intranuclear concentration measurements of doxorubicin in living leukocytes from patients treated for a lympho-proliferative disorder. *Leuk Res* 16: 647–653.
65. Long DJn, Jaiswal AK (2000). Mouse NRH: quinone oxidoreductase (NQO2): Cloning of cDNA and gene- and tissue specific expression. *Gene* 252: 107–117.
66. Wang YM, Madanat FF, Kimball JC, Gleiser CA, Ali MK, Kaufman MW, van Eys J (1980). Effect of vitamin E against adriamycin-induced toxicity in rabbits. *Cancer Res* 40: 1022–1027.
67. Prestera T, Holtzclaw WD, Zhang Y, Talalay P (1993). Chemical and molecular regulation of enzymes that detoxify carcinogens. *Proc Natl Acad Sci USA* 90: 2965–2969.
68. Inamdar NM, Ahn YI, Alam J (1996). The heme-responsive element of the mouse heme oxygenase-1 gene is an extended AP-1 binding site that resembles the recognition sequences MAF and NF-E2 transcription factors. *Biochem Biophys Res Commun* 221: 570–576.
69. Prestera T, Talalay P, Alam J, Ahn YI, Lee PJ, Choi AM (1995). Parallel induction of heme oxygenase-1 and chemoprotective phase 2 enzymes by electrophiles and antioxidants: Regulation by upstream antioxidant-responsive elements (ARE). *Mol Med* 1: 827–837.
70. Elbirt KK, Bonkovsky HL (1999). Heme oxygenase: Recent advances in understanding its regulation and role. *Proc Assoc Am Phys* 111: 438–447.
71. Vile GF, Basu-Modak S, Waltner C, Tyrrell RM (1994). Heme oxygenase 1 mediates an adaptive response to oxidative stress in human skin fibroblasts. *Proc Natl Acad Sci USA* 91: 2607–2610.
72. Tsuji Y, Ayaki H, Whitman SP, Morrow CS, Torti SV, Torti FM (2000). Coordinate transcriptional and translational regulation of ferritin in response to oxidative stress. *Mol Cell Biol* 20: 5818–5827.
73. Dorner A, Schultheiss HP (2000). The myocardial expression of the adenine nucleotide translocator isoforms is specifically altered in dilated cardiomyopathy. *Herz* 25: 176–180.
74. Van Vleet JF, Ferrans VJ, Badylak SF (1982). Effect of thyroid hormone supplementation on chronic doxorubicin (adriamycin)-induced cardiotoxicity and serum concentrations of T3 and T4 in dogs. *Am J Vet Res* 43: 2173–2182.
75. Kahl S, Elsasser TH, Blum JW (2000). Effect of endotoxin challenge on hepatic 5′-deiodinase activity in cattle. *Domest Anim Endocrinol* 18: 133–143.
76. Ito H, Miller SC, Billingham ME, Akimoto H, Torti SV, Wade R, Gahlmann R, Lyons G, Kedes L, Torti FM (1990). Doxorubicin selectively inhibits muscle gene expression in cardiac muscle cells in vivo and in vitro. *Proc Natl Acad Sci USA* 87: 4275–4279.